Translated from *Uspekhi Khimii*, **55**, 387-417 (1986) U.D.C. 541.128; 541.183; 543.422.25

# The Study of Heterogeneous Catalysis by Nuclear Magnetic Resonance

V.M.Mastikhin and K.I.Zamaraev

The use of modern NMR Fourier spectrometers to study heterogeneous catalysts and molecules adsorbed on their surface has been examined. Data obtained in the study of vanadium catalysts for the oxidation of sulphur dioxide; the state of aluminium and silicon in aluminium and silicon oxides and in zeolites; hydroxide groups; and platinum in deposited platinum catalysts, and also the first data on the $^{17}O$ NMR of oxide catalysts, have been summarised. The results of the study of adsorbed molecules, including the use of the high-resolution NMR spectroscopy of solids, have been discussed.
The bibliography contains 158 references.

CONTENTS

I. Introduction 175
II. High-resolution NMR spectroscopy in the study of solids 176
III. The study of heterogeneous catalysts 178
IV. The study of adsorbed molecules and their transformations 184

## I. INTRODUCTION

Nuclear magnetic resonance (NMR) is one of the basic modern physical methods of study in chemistry. The high sensitivity to changes in the structure of molecules and to intermolecular interactions, the possibility of quantitative analysis, and the simplicity and reliability of the interpretation of the spectra have made NMR an important instrument in the study of the structure and reactivity of substances in solution.

In homogeneous catalysis, NMR has for a long time been widely used to establish the structure of catalytically active complexes, and to study ligand exchange, intramolecular rearrangements, inner-sphere and outer-sphere coordination of solvent molecules to molecules of the catalyst, the formation of intermediate complexes between the catalyst and the substrate, etc. (see the earlier review[1] and references therein). In heterogeneous catalysis, however, NMR has until recently been much less frequently used, since the study of solid catalysts and adsorbed molecules by this method is complicated by the much larger (by a factor of approximately $10^3$–$10^4$) NMR line width in the case of solids, compared with liquids. The marked broadening of the lines, firstly, decreases sharply the sensitivity of the method and, secondly, generally leads to a loss of information on the most important characteristics of the NMR spectra, namely the chemical shifts and spin–spin coupling constants. The decrease in sensitivity is particularly marked, since heterogeneous catalysts often consist of elements for which the nuclei of the magnetic isotopes either have low natural concentrations (for example 0.037% for $^{17}O$, 8.6% for $^{119}Sn$, etc.) or have a small magnetic moment ($^{27}Al$, $^{51}V$, $^{63}Cu$, $^{65}Cu$, $^{11}B$, $^{9}Be$, $^{71}Ga$, etc.). On the other hand, the study of adsorbed molecules is often made difficult by the small quantity of the substance being studied in the specimen.

At the same time, in principle, the NMR spectra of solids carry much more information on the structure of a substance than the spectra of liquids. This is related to the fact that many interactions which are averaged in liquids as a result of the thermal motion of the molecules are fully revealed in the spectra of solids; this makes it possible to obtain valuable information on the structure of crystals and the chemical bonding in them. For example, dipole–dipole interaction is not revealed in the spectra of liquids; in the case of solids, it carries information on the relative arrangement of atoms. Analysis of the temperature dependence of the dipole contribution to the line width makes it possible to study nuclear movements of different kinds in solids. Quadrupole interactions are also averaged in liquids, but their study in solids makes it possible to obtain information on the distribution of charges around a nucleus. In the spectra of liquids, the chemical shift is described by a single parameter, namely the isotropic magnetic shielding constant, whereas in the spectra of solids it is characterised by the three components of the magnetic shielding tensor, that is it contains much more information on the chemical bond than can be obtained from the NMR spectra of liquids.

A characteristic feature of NMR spectra is that in solids the interactions of different types often have similar orders of magnitude. Thus to obtain the required information it is necessary to separate from the spectrum the parameters characterising the interactions of a definite type. This makes it necessary to carry out additional experiments involving measurements at different frequencies and over a range of temperatures, the computer calculation of spectra, etc. The development of a new generation of NMR spectrometers which make it possible to carry out measurements in strong magnetic fields (~7 T) with Fourier transformation of the NMR signal, and also the use of different methods for decreasing the line width (the high-resolution NMR spectroscopy of solids), have led to qualitative changes in the possibilities provided by NMR in the study of heterogeneous catalysts and adsorbed molecules.

Most importantly, the use of strong magnetic fields and the rapid accumulation of signals by Fourier transformation, together with the marked increase in the volume of the specimen, has led to a sharp increase in the sensitivity of the method, making it possible to proceed to systematic studies of NMR involving the nuclei of various elements present in catalysts and adsorbed molecules. Fundamentally new possibilities for the study of catalysts appeared as a result of the application of the methods of the high-resolution NMR spectroscopy of solids, such as rotation of the specimens with a high frequency at the magic angle to the external field (MAS, or VMU in Russian) and the use of pulse sequences, which lead to a decrease in the line width in the spectra of solids. The use of these methods makes it possible to average some interactions, leaving others unchanged, and hence to analyse separately interactions of different types. In a number of cases these methods make it possible to obtain spectra with a resolution comparable with that of the spectra of liquids.

This considerable expansion of the possibilities provided by the method has led to the appearance in recent years of a large number of studies of adsorption and heterogeneous catalysis by NMR spectroscopy. The present review examines the principal results of studies in this field carried out in the period 1976–1983. Earlier studies were examined in earlier reviews.[2–4] The possibilities provided at present by NMR spectroscopy in this field are demonstrated, and new data on the structure of a number of important catalysts and on the mechanisms of adsorption and catalysis, obtained by this method, are also discussed.

## II. THE HIGH-RESOLUTION NMR SPECTROSCOPY OF SOLIDS

This rapidly developing branch of NMR spectroscopy[4–10] is extending considerably the possibilities provided by the method in the study of catalysts and adsorbed molecules.

The principles of the methods of high-resolution NMR spectroscopy of solids, most frequently used in the study of catalysts and adsorbed molecules, are described below.

### 1. The Principal Interactions in NMR Spectroscopy

The Hamiltonian $\mathcal{H}$ describing the NMR effect in solids consists of several terms:[11,12]

$$\mathcal{H} = \mathcal{H}_z + \mathcal{H}_Q + \mathcal{H}_D + \mathcal{H}_\sigma + \mathcal{H}_E + \mathcal{H}_{rf} \qquad (1)$$

Here, $\mathcal{H}_z$ is the Zeeman term characterising the interaction of the magnetic moment of the nucleus with the external magnetic field; $\mathcal{H}_Q$ the Hamiltonian of the quadrupole interaction, significant for nuclei with $I > 1/2$; the spectroscopic parameters determined by this term carry information on the electric field gradient at the point where the nucleus is situated; $\mathcal{H}_D$ the Hamiltonian of the dipole–dipole interaction; the parameters determined by it carry information on the relative positions of the nuclei; $\mathcal{H}_\sigma$ the Hamiltonian of the chemical shift characterising the shielding of the nuclei by electrons; measurement of the parameters determined by this term makes it possible to identify the chemical state of the atom; $\mathcal{H}_E$ the Hamiltonian describing the interaction of the magnetic moments of the nuclei with the magnetic moments of unpaired electrons; it is important for paramagnetic materials; the parameters determined by this term contain information on the relative positions of the nuclei and the unpaired electrons and on the nature of the chemical bond; and $\mathcal{H}_{rf}$ the Hamiltonian of the radiofrequency field used to observe the NMR (and to change the average values of the other terms in Eqn.(1)).

Since the terms of the Hamiltonian (1) depend on the angular coordinates in different ways, they change in different ways under the influence of molecular motion, as a result of rotation of the specimen, or under the influence of radiofrequency pulses. These changes depend on the frequency and anisotropy of the averaging action. The main idea in the high-resolution NMR spectroscopy of solids is to apply to the system of nuclear spins a strong perturbation organised in such a way as to suppress (average) some of the interactions, and hence to make it possible to study other interactions in purer form. If different perturbations are used, it is possible in principle to obtain detailed information on each interaction separately.

Before the methods of high-resolution NMR spectroscopy are described, the principal interactions of importance for the description of the NMR spectra of solids will be examined in slightly more detail; for simplicity, the treatment will be restricted to the case of diamagnetic crystals.

#### *a) Dipole–Dipole interaction*

The Hamiltonian of the direct dipole–dipole interaction in a strong magnetic field between nuclei having magnetic moments has the form:[11]

$$\mathcal{H}_D = \sum_{i<j} \frac{1}{2} \gamma_i \gamma_j \hbar^2 r_{ij}^{-3} (1 - 3\cos^2\theta_{ij}) [\vec{\mu}_i \vec{\mu}_j - 3(\mu_z)_i (\mu_z)_j] \qquad (2)$$

Here, $\gamma_i$ and $\gamma_j$ are the gyromagnetic ratios of the nuclei $i$ and $j$; $r_{ij}$ the distance between the nuclei; $\theta_{ij}$ the angle between the direction of the external magnetic field and the vector joining the nuclei $i$ and $j$; $\vec{\mu}_i$ and $(\mu_z)_i$ the vector of the magnetic moment of the nucleus $i$ and its projection on the direction of the external magnetic field; and $h$ Planck's constant. The Hamiltonian of the dipole–dipole interaction depends markedly on the relative positions of the nuclei, so that the spectroscopic parameters characterising this interaction carry information on the relative positions of the nuclei in the solid. Movement of the nuclei leads to a change in $\mathcal{H}_D$ with time, and may change the NMR spectrum (if the frequency of the motion is sufficiently high). Thus the dipole–dipole interaction is also used to study dynamic processes in solids (diffusion, restricted rotation, etc.).

Studies using direct dipole–dipole interaction to obtain information on the positions of nuclei and on their motion in solids until recently made up the greater part of studies on the NMR spectroscopy of solids. In practice, however, the data obtained can be interpreted quantitatively in terms of interatomic distances usually only for solids with a simple structure or in those cases where the solid contains isolated groups consisting of a small number of nuclei, for which the Hamiltonian has a comparatively simple form. With increase in the number of interacting nuclei, the form of the spectrum becomes much more complicated, and its width increases. As a result of the strong orientational dependence of the Hamiltonian $\mathcal{H}_D$, the broadening of the spectra is particularly marked for polycrystalline specimens; in these cases the NMR spectrum is most frequently characterised by only a single parameter, the second moment of the spectrum. This field of study of usually called low-resolution NMR spectroscopy or broad line NMR spectroscopy.

#### *b) Chemical shielding*

The movement of the electrons surrounding the nucleus produces an additional magnetic field, which, combined with the external magnetic field $H_0$, creates an effective field $H_{\text{eff}}$ at the point where the nucleus is situated.[11] To take account of this fact, the magnetic shielding tensor $\hat{\sigma}$ is introduced into the expression for the Hamiltonian of the chemical shift:

$$\mathcal{H}_\sigma = -\mu(1 - \hat{\sigma}) H_0 \qquad (3)$$

The magnetic shielding tensor is a tensor of second rank; it is often also called the chemical shift tensor. It contains information on the electronic environment of the nucleus and on the chemical bonding in the crystal. The chemical shift tensor is described by six independent parameters—the three principal values of the tensor and the three angles which characterise the positions of the principal axes of the tensor relative to the axes of the crystal. It is possible to obtain all of these quantities only from the NMR spectra of single crystals. The spectra of polycrystalline specimens can give only three parameters—the principal values of the tensor $\hat{\sigma}$.

Systematic measurements of chemical shift tensors for solids became possible only after the development of the methods of high-resolution spectroscopy, since the chemical shifts are usually smaller than the dipole broadening, and therefore do not appear when ordinary methods are used to record the NMR spectra of solid specimens. In liquids, where the rapid molecular motion averages the dipole interactions, there are no obstacles to the measurement of the chemical shifts. The molecular motion averages the chemical shift tensor in such a way that only its average value is measured; even the average value of the tensor, however, is exceptionally informative.

The methods of the NMR spectroscopy of solids make it possible to measure all three principal values of the tensor $\hat{\sigma}$, so that more information is obtained. For example, the deviation of the electron density distribution round the nucleus from spherical symmetry is reflected in the difference between the principal values of $\hat{\sigma}$, whereas the average value of the chemical shift carries only indirect information on this deviation. In addition, measurements of the temperature dependence of the anisotropy of $\hat{\sigma}$ make it possible to detect and study various movements within solids, in particular anisotropic movements.

*c) Quadrupole interaction*

The Hamiltonian of the quadrupole interaction carries information on the electric field gradient $V$ at the point at which the nucleus with $I > 1/2$ is situated:[11]

$$\mathcal{H}_Q = \frac{e^2qQ}{4I(2I-1)}[3\hat{I}_z^2 - \hat{I}^2 + \eta(\hat{I}_x^2 - \hat{I}_y^2)] \qquad (4)$$

Here, $eq = V_{zz}$, $\eta = (V_{xx} - V_{yy})/V_{zz}$, and $eQ$ the quadrupole moment of the nucleus; the $z$ axis is directed along the external magnetic field $I_+ = I_x + iI_y$. The energy of the quadrupole interaction is usually much lower than the energy of the Zeeman interaction, and the influence of the quadrupole interaction on the spectra is revealed in first- and second-order perturbation theory. In first-order perturbation theory, the Zeeman levels are displaced by an amount which depends on the projection of the magnetic moment of the nucleus on the direction of the external field. This leads to the appearance of $2I$ lines in the NMR spectrum. For nuclei with half-integral spins, the central transition ($-1/2 \leftrightarrow 1/2$) remains unchanged in first-order perturbation theory. In second-order perturbation theory, the central transition is split, and its centre of gravity is displaced; the values of the splitting and the shift are inversely proportional to the magnitude of the external magnetic field.

The Hamiltonian of the quadrupole interaction may be so large that the displacements of second order will be close to (or greater than) the values of the chemical shift and the dipole contribution to the line width, particularly for measurements at low frequencies. The main difficulty in the recording of the NMR spectra when there are large quadrupole contributions is due to the marked broadening of the lines as a result of the non-uniformity of the electric field at different points in the specimen, and also as a result of the angular dependence of the energy of the quadrupole interaction (in the case of polycrystalline specimens). In these cases, for nuclei with half-integral spins, information can be obtained from measurements of second-order effects for the central transition.

## 2. Methods for Decreasing the Line Widths in the Spectra of Solids

*a) Rotation of the specimen at the magic angle*

Rapid rotation of the specimen about an axis directed at the so-called "magic" angle of 54°44', to the external magnetic field may lead to a considerable decrease in the line widths in the NMR spectra.[9,13-17] This follows from an examination of the expressions describing the Hamiltonians $\mathcal{H}_D$, $\mathcal{H}_\sigma$, and $\mathcal{H}_Q$ in Eqn.(1).

The Hamiltonian of the dipole–dipole interaction (2) can be considered first. When the specimen is rotated, the angle $\theta_{ij}$ between the external magnetic field and the vector $\vec{r}_{ij}$ depends on time, and the difference $(1 - 3\cos^2\theta_{ij})$ takes both positive and negative values. Analysis of expression (2) shows that rotation of the specimen about an axis coinciding with the direction of the field has no influence on the spectrum; rotation about an axis perpendicular to the field decreases the line width by a factor of 2; and rotation about an axis making an angle of 54°44' with the direction of the field ($\cos^2 54°44' = 1/3$) averages the dipole–dipole interaction to zero. The physical significance of this phenomenon is that when the rotation is sufficiently rapid, so that $h\nu$ (where $\nu$ is the frequency of the rotation, and $h$ is Planck's constant) is greater than the energy of the dipole–dipole interaction, the nuclei "feel" only the average value of the energy of the dipole–dipole interaction, which is equal to zero when the specimen is rotated at the magic angle. This leads to a marked decrease in the line width. On the other hand, as shown in Ref.13, the second moment of the spectrum remains unchanged when the specimen is rotated at the magic angle. As a result, the spectrum consists of a narrow central line and a system of side bands separated from it by distances which are multiples of the frequency of rotation.

Similarly, rapid rotation at the magic angle also averages the anisotropy of the chemical shift, giving an isotropic spectrum with an average value $\sigma = 1/3(\sigma_{zz} + \sigma_{yy} + \sigma_{xx})$.

The first-order quadrupole interaction is also effectively averaged when the specimen is rotated at the magic angle.[15] In contrast to this, the second-order quadrupole interaction is not completely averaged when the specimen is rotated in this way. In a number of cases this makes it difficult to obtain well resolved spectra.

The influence of molecular motion on the efficiency of the decrease in the line width as a result of rotation of the specimen at the magic angle has been studied.[17] The possibility of decreasing the line width depends on the type of molecular motion. If there is rapid restricted motion, for example random reorientation of the molecules or individual functional groups about a single axis, there is a partial decrease in the line width, and rapid rotation at the magic angle averages the remaining broadening. If however the molecular motion is completely random, but its rate is not sufficient to give narrow lines with widths close to the line widths in the spectra of liquids, then rotation of the specimen with a frequency of several kilohertz does not lead to a decrease in the line width. A decrease in width takes place if the frequency of the rotation is higher than the frequency of the molecular motion, which in most cases cannot be achieved in practice. This limitation in the production of high-resolution spectra also applies to other methods for decreasing the line widths in the spectra of solids.[2-5]

*b) Multi-pulse sequences*

In the case of very strong dipole interactions, when rotation of the specimen at the magic angle at attainable rates gives no result, the line width can be decreased using multi-pulse sequences.[2-5] In a multi-phase experiment, a four-pulse cycle is usually employed.[5] As a result, the average values of the Hamiltonians of the dipole and quadrupole interactions become zero. When a sequence of radiofrequency pulses is applied to a spin system, the nuclear spins begin to rotate about an axis making the magic angle with the direction of the field, and in the rotating system of coordinates the vector of the magnetisation of the system is oriented at this angle to the external field. As a result, the dipole–dipole interactions disappear. The Hamiltonian of the dipole interaction (2) can be represented as:

$$\mathcal{H}_D = \sum_{i<j} \gamma_i\gamma_j\hbar^2 r_{ij}^{-5}(\vec{r}_{ij}\vec{r}_{ij} - 3z_{ij}z_{ij})\,[\vec{\mu}_i\vec{\mu}_j - 3\,(\mu_z)_i\,(\mu_z)_j] \qquad (5)$$

In expression (5) the dependence of $\mathcal{H}_D$ on the coordinates of the vector $\vec{r}_{ij}$ and its dependence on the orientation of the spin moments are identical, so that rotation of the specimen and rotation of the nuclear spins at the same angle to the direction of the field lead to the same result.

The application of an appropriately selected sequence of radiofrequency pulses can reduce to zero not only the dipole–dipole interaction but also the first-order quadrupole interaction.[5] The effects of the chemical shift are preserved, although they are decreased by a factor of $3^{1/2}$, since the projection of the magnetisation vector on the direction of the external field is reduced by this factor. The spin–spin interaction via the chemical bond, which is independent of the magnitude of the angle, remains unchanged. Thus a sequence of radiofrequency pulses can be used to obtain high-resolution NMR spectra for solid specimens.

The efficiency of the decrease in the line width in multi-pulse experiments depends to a marked extent on the accuracy of the tuning of the pulses. Such factors as the finite length of the pulses, the non-uniformity of the radiofrequency field, the inaccuracy of the tuning of the phases, and the distortion of the form of the pulses have a marked influence on the width of the spectra obtained. These difficulties can be partly overcome by using complex sequences.[18,19] Almost all more complex pulse sequences are based on the four-pulse sequence in such a way that the experimental errors do not accumulate from one cycle to another.

The influence of various factors on the effective line width in multi-pulse experiments has been analysed;[18,19] it has been shown that the form of the high-resolution spectrum depends to a marked extent on the conditions of the experiment and even on the actual magnitude of the chemical shift. This may make it difficult to interpret the spectra and to determine the components of the shielding tensor. Another problem is that multi-pulse experiments do not completely eliminate heteronuclear dipole interactions, that is interactions between nuclei of different types. Like the anisotropy of the chemical shift, the heteronuclear dipole interaction decreases by a factor of $3^{1/2}$ in a four-pulse experiment. To suppress this interaction, it is necessary to use methods based on double resonance, for example cross polarisation.

*c) Cross polarisation*

Cross polarisation[20] is most widely used to obtain high-resolution spectra for $^{13}C$ nuclei. The method not only suppresses dipole interactions but also increases the intensity of the $^{13}C$ NMR signals by a factor of ~4 as a result of the transfer of polarisation from protons to carbon nuclei.

The first experiments to record NMR spectra using cross polarisation were described in Refs. 21 and 22. The method was subsequently improved considerably,[20] when it was shown experimentally that it is possible to suppress the scalar spin–spin and dipole interactions between spins of two kinds ($I_1$ and $I_2$) by recording the NMR spectrum of the spins $I_1$ under conditions in which the spins $I_2$ are irradiated by a strong electromagnetic field whose frequency is equal to their Larmor frequency. Under these conditions, not only are the scalar and dipole interactions between the spins $I_1$ and $I_2$ suppressed, but the relaxation time for the nuclear spins $I_1$ may also be decreased as a result of the exchange of energy between them. The recording time of the spectrum of the nuclei $I_1$ is preserved, so that the sensitivity of the method is increased as a result of accumulation of the signal.

In cross polarisation experiments, the scalar spin–spin and dipole interactions are completely suppressed, whereas the anisotropy of the chemical shift remains unchanged, so that it can be studied in pure form. As a rule, for $^{13}C$ nuclei the difference between the components of the chemical shift tensor reaches several hundred p.p.m. As a result, the spectrum is extended considerably over a wide frequency range. In this case it is possible to use a combination of cross polarisation and rotation of the specimen at the magic angle. This method often makes it possible to obtain for solid specimens spectra whose resolution is comparable with that of the spectra of liquids.

Thus special methods (rotation of the specimen at the magic angle, multi-pulse sequences, and cross polarisation) can suppress the interactions leading to line broadening and hence give high-resolution spectra for solids. The suppression of second-order quadrupole interactions presents the greatest difficulties. Here, the principal method involves increasing the resonance frequency by using stronger magnetic fields. It is also possible to use a method based on the recording of many-quantum transitions between levels which are not influenced by first-order quadrupole effects.[23-27] Dipole–dipole interactions can be suppressed fairly frequently by the above methods involving rotation at the magic angle, multi-pulse sequences, and cross polarisation.

## III. THE STUDY OF HETEROGENEOUS CATALYSTS

This section examines the results of the study of the structure of heterogeneous catalysts and their active centres by NMR involving the nuclei of different elements and the methods for decreasing the line width described in the previous section.

### 1. The $^{51}V$, $^{17}O$, and $^{23}Na$ NMR Study of Vanadium Catalysts for the Oxidation of Sulphur Dioxide

Oxygen-containing compounds of vanadium form part of many industrially important oxidation catalysts. The structure of the active centres and the mechanisms of the action of these catalysts have been insufficiently studied, however. The present section demonstrates for the example of catalysts for the oxidation of sulphur dioxide the possibilities provided by NMR using the nuclei of $^{51}V$ (natural abundance ~100%) and various other elements in the study of the structure and mechanisms of the production of vanadium catalysts.

The catalysts used to oxidise sulphur dioxide are sulphate and pyrosulphate compounds of vanadium and alkali metals, deposited on a porous carrier, usually silica gel or an aluminosilicate. X-Ray diffraction has shown that in these compounds, vanadium is surrounded by oxygen atoms forming a regular or distorted tetrahedron or a distorted octahedron.

$^{51}V$ NMR spectra recorded at low frequencies usually have a very complex form, because of the simultaneous influence of dipole and quadrupole interactions and chemical shift effects, which may be of the same order of magnitude.[28] On going to high resonance frequences $\nu_0 \cong 79$ MHz, achieved by using magnets with a field $H_0 \cong 7$ T, however, the influence of second-order quadrupole effects becomes insignificant, the spectra become much simpler, and it becomes possible to measure the anisotropy of the chemical shift.

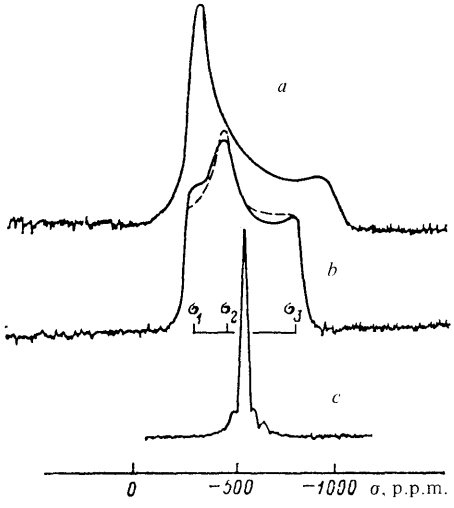



**Figure 1.** $^{51}V$ NMR spectra of vanadium compounds with different oxygen environments; the chemical shifts are given relative to $VOCl_3$;[29] *a*) $V_2O_5$ (distorted octahedron), *b*) $KVO_3$ (distorted tetrahedron), *c*) $K_3VO_4$ (regular tetrahedron).

The spectra of a number of individual vanadium compounds with known structures were studied first,[29] and it was shown for a large number of these model compounds that the anisotropy of the chemical shift can be taken as a characteristic of the structure of the oxygen environment of the vanadium atoms. Fig.1 shows typical $^{51}V$ NMR spectra for vanadium atoms in a regular tetrahedral environment (orthovanadates and pyrovanadates), in a distorted tetrahedral environment (metavanadates), and in a bipyramidal (distorted octahedral) environment (vanadium pentoxide, sulphate vanadates). For ortho- and pyrovanadates, the spectrum is almost isotropic. The spectrum of metavanadates indicates triaxial anisotropy of the chemical shift tensor (the corresponding spectrum, obtained by calculation using the optimally selected values of $\sigma_1$, $\sigma_2$, and $\sigma_3$, is given by the broken line in Fig.1). Vanadium in a bipyramidal environment gives spectra with almost axial symmetry of the tensor $\sigma$. For alkali metal metavanadates, a correlation is observed between the anisotropy of the chemical shift and the degree of distortion of the tetrahedron.[29]

The $^{51}V$ NMR spectra of different industrial catalysts for the oxidation of $SO_2$ (KS, BAV, and IK-1 grades) before the catalytic reaction differ considerably and depend on the method used to prepare the catalyst. Treatment of the catalysts under the conditions of the catalytic reaction, however, smooths out these differences to a considerable extent.[30] Thus in all the catalysts studied, the active component is produced in the course of the actual catalytic reaction. Although the chemical character of the compounds responsible for the catalytic properties of vanadium catalysts has not yet been finally determined, some preliminary conclusions can be reached. Thus comparison of the $^{51}V$ NMR spectra of the catalysts with the spectra of sulphate vanadates (see Fig.2) shows that one of the principal components of the industrial catalysts is the sulphate vanadate $K_3VO_2SO_4S_2O_7$.

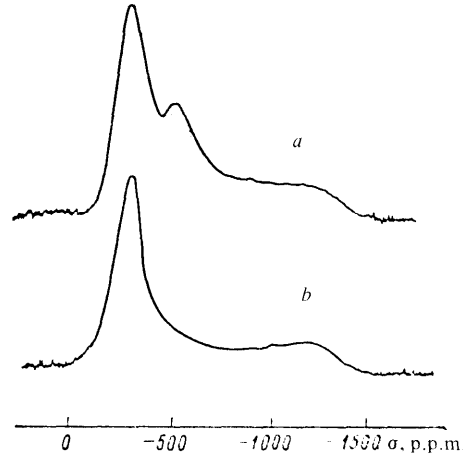



**Figure 2.** Comparison of the spectrum of the IK-1 catalyst for the oxidation of sulphur dioxide (*a*) with that of the potassium sulphate vanadate $K_3VO_2SO_4S_2O_7$ (*b*); the chemical shifts are given relative to $VOCl_3$.[31]

In addition to the lines from potassium sulphate vanadate, the spectra of the industrial catalysts usually show a line with $\sigma \cong -500$ p.p.m. relative to $VOCl_3$, characteristic of vanadium atoms in a regular tetrahedral environment (see Fig.2). This line has been assigned to vanadium atoms interacting with the carrier, silica gel or an aluminosilicate.[31] Thus vanadium pentoxide deposited on silica gel gave the same line;[31] its intensity increased with increase in the surface area of the silica gel for a constant quantity of vanadium pentoxide. Thus the carrier reacts chemically with the active component. Reactions of this type may be responsible for the fact that the catalytic activity depends on the type of carrier.

The spectra in Figs.1 and 2 were recorded at room temperature, at which the active component of the catalysts and the model compounds are solid. Under the conditions of the oxidation of sulphur dioxide (400–500 °C), however, the active component of the catalysts is in the molten state, and forms a very thin liquid film on the solid carrier. The chemical composition of the catalysts cooled to room temperature may differ from the composition at a high temperature. The spectra of the vanadium catalysts were therefore studied at 500 °C in an atmosphere of the reaction medium.[32]

The $^{51}V$ NMR spectra could not be observed at this temperature, because of the large width, apparently due to the short spin–lattice relaxation time of the vanadium nuclei. The melts were therefore studied by $^{17}O$ and $^{23}Na$ NMR. Fig. 3 gives the concentration dependence of the chemical shift and the line width for the $^{17}O$ NMR spectrum of vanadium pentoxide–potassium pyrosulphate melts, kept for a long time at 500 °C in an atmosphere of the equilibrium mixture $SO_3 \rightleftarrows SO_2 + \frac{1}{2}O_2$ at an $SO_3$ pressure of 400 mmHg.[32] The chemical shift and the line width depend markedly on the concentration of vanadium in the melt. This shows that a coordinate bond is formed between the pyrosulphate or sulphate anions and the vanadium cations. The nature of the relationships in Fig. 3 can be explained if it is assumed that in the melt there is exchange between sulphate and pyrosulphate anions not combined with vanadium and anions forming a coordinate bond with vanadium. The change in the slope of the lines in Fig. 3 at a vanadium concentration of ~1 M reflects a change in the state of the vanadium complexes, possibly as a result of their dimerisation.

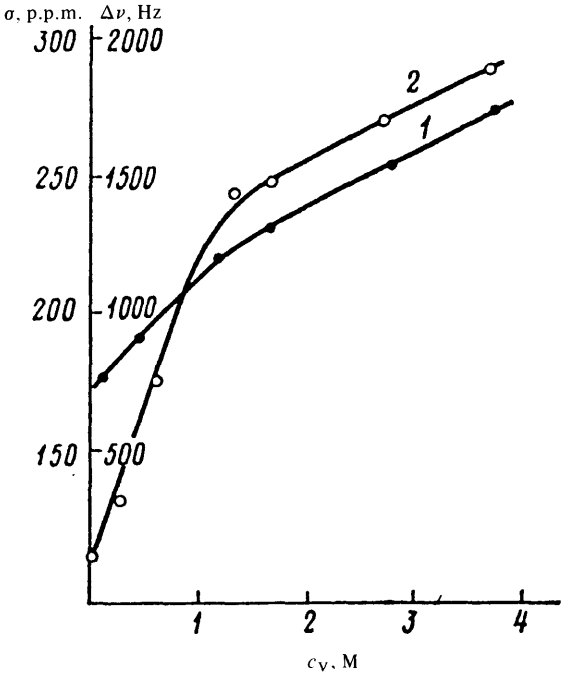



**Figure 3.** Dependence of the chemical shift σ (*1*) and the line width Δν (*2*) of the $^{17}O$ NMR spectra of the $K_2S_2O_7$–$V_2O_5$ system (500 °C, $SO_3$, $SO_2$, $O_2$ atmosphere) on the vanadium concentration; the chemical shift was measured relative to $H_2O$ at 25 °C.[32]

The replacement of potassium by sodium makes it possible to study the $^{23}Na$ NMR spectra of these melts.[32] Fig. 4 gives as a typical example the dependence of the $^{23}Na$ chemical shift on the ratio of the concentrations of sodium and vanadium, obtained for vanadium pentoxide–sodium pyrosulphate melts at 500 °C. These data indicate that sulphate (or pyrosulphate) compounds of vanadium are coordinated to some of the sodium cations. The relatively small changes in σ and the small line width (~300 Hz) agree satisfactorily with the model of outer-sphere coordination of the sodium ions.

Thus the study of vanadium catalysts for the oxidation of $SO_2$ shows that $^{51}V$ NMR can be used successfully to identify the vanadium compounds in heterogeneous catalysts and to detect chemical interaction between the active component and the carrier. $^{17}O$ NMR, even at the natural concentration of this isotope (0.037%), makes it possible to study melts of the active component of the catalyst directly under the conditions of the catalytic reaction.

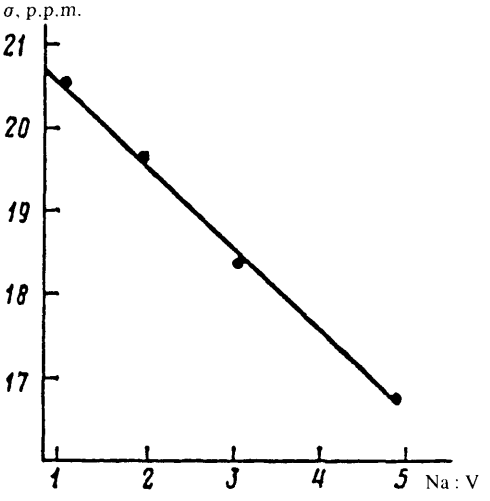



**Figure 4.** Dependence of σ on the ratio Na : V for an $Na_2S_2O_7$–$V_2O_5$ melt at 500 °C; the chemical shift was measured relative to NaCl.[32]

### 2. $^{27}Al$ NMR Studies of the State of Aluminium in Aluminium Oxides and Zeolites

Aluminium in an oxygen atom environment is present in many industrial catalysts. There is good evidence that it is often present in their active centres. The study of the state of aluminium in catalysts from the $^{27}Al$ (natural abundance 100%) NMR spectra is therefore of undoubted interest.

The spin of the $^{27}Al$ nucleus is 5/2. The $^{27}Al$ NMR spectra of powders usually show only the line from the central transition ($1/2 \leftrightarrow -1/2$), whose position is determined by the chemical shift and the second-order quadrupole effect. With increase in the working frequency ($\nu_0$), the chemical shifts increase in direct proportion to $\nu_0$, and the second-order quadrupole shifts decrease in inverse proportion to $\nu_0$. For example, for powdered zeolites and crystalline aluminium oxides even at $\nu_0 \cong 78$ MHz (magnetic field 7 T), the second-order shifts are much smaller than the line widths and the typical chemical shifts produced as a result of a change in the symmetry of the oxygen environment of the aluminium ions. The chemical shifts of aluminium in tetrahedral and octahedral oxygen environments in solution differ by 80 p.p.m.[33] For solids, the magnitude of σ also characterises the coordination state of aluminium, whereas the quadrupole coupling constant depends little on the aluminium coordination (oxygen tetrahedra or octahedra).[34] When the specimens are rotated at the magic angle, it is possible to obtain high-resolution $^{27}Al$

NMR spectra and to observe separately in these spectra the lines from aluminium in tetrahedral and octahedral oxygen environments. Methods for analysing the high-resolution NMR spectra for nuclei with a quadrupole moment have been developed,[35-38] and the principal methods for extracting the spectral parameters from the spectra of nuclei with a spin $I > 1/2$ have been described.

The review of the results of the study of the state of aluminium in heterogeneous catalysts by $^{27}Al$ NMR can begin with an examination of aluminium oxides.[39] Fig. 5 gives the spectra of powdered specimens of different crystalline aluminium oxides, and shows that rotation of the specimens at the magic angle leads to a marked decrease in the line width. For example, for γ-alumina the line width decreases by a factor of 6, and the two lines corresponding to tetrahedral and octahedral coordination of the aluminium atoms are resolved. Comparison of their positions with those of the lines for model oxygen-containing compounds of aluminium makes it possible to assign the weak-field line to aluminium atoms in a tetrahedral oxygen environment, and the strong-field line to atoms in an octahedral environment. This assignment is confirmed by the spectrum of α-alumina, which, as expected from the known structure of this compound, consists of a single line whose chemical shift corresponds to that of aluminium atoms in octahedral coordination. The comparatively good resolution of the spectra makes it possible in principle to determine the relative concentrations of aluminium in octahedral and tetrahedral oxygen environments. Accurate quantitative measurements are difficult, however, since the rotation of the specimens leads to the appearance of side bands which partly overlap the line from the "tetrahedral" aluminium atoms. The side bands are marked with asterisks in Fig. 5.

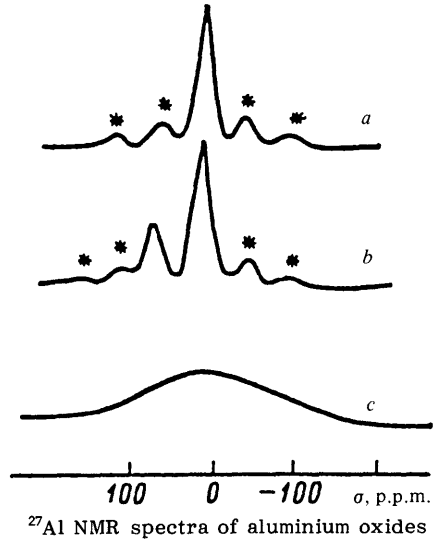



**Figure 5.** $^{27}Al$ NMR spectra of aluminium oxides with rotation of the specimen at the magic angle: *a*) α-$Al_2O_3$, *b*) γ-$Al_2O_3$; *c*) γ-$Al_2O_3$ without rotation; the chemical shift was measured relative to $Al(H_2O)_6^{3+}$.[39]

In the case of zeolites, the lines from aluminium atoms in tetrahedral and octahedral oxygen environments can be resolved even without rotating the specimens at the magic angle.[30] The $^{27}Al$ NMR spectra[30] show that on hydrothermal treatment of $NH_4Y$ zeolite, which gives HY zeolite, some of the aluminium ions leave their tetrahedral positions in the zeolite lattice and move into cavities where they acquire octahedral coordination. Treatment of the specimens at a high temperature leads to breakdown of the zeolite structure, and a broad line appears in the spectrum.

Measurements of the integral intensity of the $^{27}Al$ NMR spectra have made it possible to determine the relative numbers of aluminium atoms remaining in the lattices of zeolites of types A and Y and displaced into cavities as a result of different forms of hydrothermal treatment and subsequent dehydration of the zeolites.[40,41] The zeolite specimens were placed in a solution of acetylacetone in ethanol, and the intensity of the broad signal from the aluminium atoms remaining in the lattice was compared with that of the narrow signal from the mobile aluminium atoms in the cavities. It was found that only a small proportion of the aluminium atoms (~10%) is displaced from the lattice when the specimens are treated in a shallow bed. When the specimens are treated in a deep bed, the number of aluminium atoms displaced from the lattice increases with increase in temperature. Thus after treatment of the specimens at 400 °C in a deep bed, ~50% of the aluminium atoms were displaced from the lattice. The high-resolution $^{27}Al$ spectra of zeolites which had been rehydrated after hydrothermal treatment and dehydration contained an additional line from the atoms of mobile hydrated aluminium displaced from the lattice. The proportion of this form of aluminium amounted to 70% of the total aluminium displaced from the zeolite framework after treatment at 300 °C. Increase in the temperature of treatment to 700 °C lowered this fraction to 3%. Comparison of the intensity of the $^{27}Al$ NMR lines with that of the $^{1}H$ NMR signals from the OH groups after treatment of the catalysts at different temperatures shows that the zeolite dehydroxylation scheme[42] which assumes that three-coordinate aluminium is formed is incorrect. In fact, dehydroxylation in water vapour takes place at the same time as the removal of aluminium.[40]

Comparison of the $^{27}Al$ NMR spectra of A, X, and Y zeolites established that the A zeolite does not contain Al–O–Al bonds; this confirmed that A zeolite obeys Loewenstein's rule.[43]

Thus the study of the high-resolution $^{27}Al$ spectra makes it possible to determine the coordination state of aluminium in oxides and zeolites and to follow the process of the removal of aluminium from zeolites. Further increase in the working frequency of the spectrometers should make it possible to use the $^{27}Al$ NMR spectra to distinguish tetrahedral aluminium atoms occupying different positions in a zeolite structure.

### 3. $^{29}Si$ NMR Studies of the State of Silicon in Silicate Systems

Silicon oxides, like aluminium oxides, are widely used in heterogeneous catalysis. The $^{29}Si$ isotope (natural abundance 4.7%) has a nuclear spin $I = 1/2$. There are therefore no quadrupole effects in $^{29}Si$ NMR spectra, so that it is usually simpler to obtain high-resolution NMR spectra of solid specimens for $^{29}Si$ nuclei, than for $^{27}Al$ nuclei.

One of the first applications of $^{29}Si$ NMR to the study of catalysts was an investigation of the surface of silica gel using cross polarisation and rotation of the specimen at the magic angle.[44] The use of these methods made it possible to observe in the spectra of silica gel lines with chemical shifts of −109.3, −99.8, and −90.6 p.p.m. relative to tetramethylsilane (TMS), whose intensities changed to different extents

with the transfer of polarisation from the protons to the silicon nuclei. From a comparison of these spectra with the spectra of silicate solutions, the lines with chemical shifts of −99.8 p.p.m. and −90.6 p.p.m. were assigned to the structures $HOSi(SiO_4)_3$ and $(HO)_2Si(SiO_4)_2$, and the line at −109.3 p.p.m. to $Si(SiO_4)_4$ groups. The first two structures correspond to surface silicon atoms joined to one or two hydroxide groups, and the third corresponds to silicon atoms in the volume. These results show that NMR can be used to distinguish chemically non-equivalent silicon atoms, and also surface and volume silicon atoms, in catalysts.

This approach was subsequently used to study the dehydration and rehydration of silica gel.[45] These processes depend markedly on the relative arrangement of the OH groups; $^{29}Si$ NMR was used to determine the quantity of geminal groups, that is structures of the type $(HO)_2Si(SiO_4)_2$. The results[45] showed that none of the previously proposed models explains all the regular features of the change in the structure of the surface during dehydration and rehydration. It was found that the silica gel surface is non-uniform, and may contain regions with structures resembling the (111) and (100) faces of cristobalite. It was concluded[45] that on regions of both types, the rehydration process is determined by kinetic rather than thermodynamic factors.

The possibilities provided by high-resolution $^{29}Si$ NMR spectroscopy for the determination of the ordering of silicon in silicates with different compositions have been demonstrated.[46] The $^{29}Si$ NMR spectra of the solutions and solids are similar, and depend on the condensation of the $SiO_4^{4-}$ tetrahedra. In aluminosilicates, the chemical shifts change regularly with change in the degree of replacement of silicon by aluminium in the tetrahedra closest to the $SiO_4^{4-}$ tetrahedron being considered. The spectra obtained for zeolites of type A showed that each $SiO_4^{4-}$ tetrahedron is surrounded by three $AlO_4^{5-}$ tetrahedra and one $SiO_4^{4-}$ tetrahedron, and that each $AlO_4^{5-}$ tetrahedron is surrounded by three $SiO_4^{4-}$ tetrahedra and one $AlO_4^{5-}$ tetrahedron (3 : 1 ordering). This arrangement of the tetrahedra does not obey the rule of alternation of aluminium–oxygen and silicon–oxygen tetrahedra (Lowenstein's rule,[43] noted above). It was therefore suggested[47] that the previously adopted model of the structure of the A zeolite is incorrect, and neutron diffraction and high-resolution electron microscope data were used to propose a new model for the structure of the A zeolite, containing Al–O–Al bonds.[47] This raised the question of the extent to which Loewenstein's rule can be used to analyse the distribution of aluminium in other zeolites.[48] Suggestions have been put forward on the possible reasons for the breakdown of this rule.

Subsequently, a more detailed study of the NMR spectra of ZK-4 zeolites, in which the aluminium atoms, as in the A zeolite, are present in double four-membered rings, showed that the $^{29}Si$ NMR spectrum depends not only on the number of neighbouring $AlO_4^{5-}$ groups but also on the Si–O–Si or Si–O–Al angle.[49] It was found that the strain of the bonds in structures with four-membered rings, which contain almost linear Si–O–Al bonds, leads to a displacement of the resonance compared with other structures with the same chemical composition. As a result, the signals which were previously assigned to Si atoms having three Al atoms in the second coordination sphere were found to belong to an Si atom joined to four Al atoms in neighbouring tetrahedra, as should be the case for a zeolite A structure obeying Loewenstein's rule.

The distribution of aluminium in X and Y zeolites has been studied in detail,[50,51] and it has been shown that the regular features of the change in the intensities of the lines in the $^{29}Si$ NMR spectra with change in the aluminium concentration obey Loewenstein's rule.

$^{29}Si$ NMR spectroscopy has been used[30,52] to study the displacement of aluminium atoms from the framework of zeolites of type Y on hydrothermal treatment. The high-resolution spectra of specimens from which aluminium ions have been displaced consist of four lines with $\sigma$ from −85 p.p.m. to −105 p.p.m. relative to TMS.[30] According to Ref.46, these lines correspond to Si atoms having 3, 2, 1, and 0 Al atoms in the second coordination sphere. Removal of ammonium ions from the zeolite leads to an increase in the intensity of the lines corresponding to the Si atoms with a smaller number of Al atoms in the second coordination sphere, and to a decrease in the intensity of the lines corresponding to a larger number of Al atoms in the second coordination sphere. This behaviour of the $^{29}Si$ NMR spectra confirms the displacement of the aluminium atoms from the zeolite lattice, detected from the $^{27}Al$ NMR spectra (see previous section).[30,52]

The $^{29}Si$ NMR spectra of Y zeolites from which aluminium ions had been displaced by thermochemical treatment in the presence of water vapour have been studied.[53] The spectra were used to calculate the concentration of $Si(O_4Si)_{4-n} \cdot (O_4Al)_n$ groups. The results show that the rate of the removal of aluminium increases with increase in the degree of replacement of $Na^+$ by $NH_4^+$ in the original specimens, and also with increase in the temperature of treatment and the partial pressure of water vapour.

The distribution of aluminium and silicon in the lattices of zeolites from which aluminium has been displaced influences their catalytic activity, adsorbing power, acidity, stability, etc. If the displacement of aluminium takes place at a sufficiently high temperature, the distribution of silicon and aluminium depends chiefly on the final ratio of the numbers of Si and Al atoms in the lattice, and not on the conditions and type of process involved in the displacement of aluminium.[54] For a given Si/Al ratio, the aluminium distribution was the same in zeolites obtained by direct synthesis and in specimens obtained by displacing aluminium, which had a higher initial aluminium concentration. Thus the final distribution of silicon and aluminium is not sensitive to the conditions of preparation of the specimen, and is determined by the minimum energy of the entire lattice. This indicates that there is a redistribution of the Si and Al atoms in the zeolite during the displacement of aluminium. If however the displacement of aluminium is carried out at relatively low temperatures, the lattice vacancies formed by the displacement of Al atoms are not occupied by Si atoms, and close to these vacancies there are four hydroxide groups (apparently one OH group next to each of the four neighbouring Si atoms). This follows from cross-polarisation experiments which showed an increase in the strength of the signals from Si atoms having one neighbouring OH group.[55]

The $^{29}Si$ NMR spectra have been used[56] to study the state of silicon in the lattices of ZSM-5 and ZSM-11 zeolites with different aluminium concentrations (the Si/Al ratio was varied from 30 to 1000). The line with $\sigma = -105$ p.p.m. was assigned to Si atoms joined to one Al atom in the second coordination sphere, since the intensity of this line decreased with decrease in the quantity of aluminium in the zeolites. The intensity of the line with $\sigma = -115$ p.p.m. in the spectra of the ZSM-11 zeolites was double that for the ZSM-5 zeolites. This made it possible to assign this line to Si atoms in four-membered rings, since the unit cell of the ZSM-5 zeolite contains four four-membered rings, and the unit cell of the ZSM-11 zeolite contains eight four-membered rings. The line with $\sigma = -103$ p.p.m. in the spectra of the ZSM-11 zeolites was assigned to silanol groups Si–OH. It was suggested[56] that the replacement of silicon by aluminium in these zeolites takes place in five-membered rings.

Thus high-resolution $^{29}Si$ NMR spectroscopy makes it possible to distinguish and identify different states of silicon in silicate structures, to obtain data on the distribution of silicon in zeolites, and to study surface Si atoms in silica gel and zeolites.

### 4. $^{195}Pt$ NMR Studies of Deposited Platinum

Since catalysts based on platinum are widely used in many industrial processes, the first papers on the use of $^{195}Pt$ NMR to study highly dispersed platinum deposited on aluminium oxide[57–59] are of considerable interest.

The $^{195}Pt$ nucleus (natural abundance 33%, spin 1/2) has the greatest Knight shift (3.37%) among metals, and this makes it possible to observe separately the signals from surface platinum atoms bonded to the carrier or to adsorbed molecules and from metallic platinum atoms in the volume. The very wide range of values of $\sigma$, the appreciable anisotropy of the chemical shift tensor, and the existence of platinum in a number of states on the surface are responsible for the appearance in the spectrum of a broad line from surface platinum atoms (~0.45 T). This is approximately $10^3$ times the typical line width in the spectra of solids. These exceptionally broad and therefore low-intensity lines have been recorded by accumulating the spin echo signals at a constant frequency with a gradual change in the magnetic field. Specimens with a platinum concentration of ~10% containing platinum particles with different dimensions were studied.[57] It was found that the form of the NMR line depends markedly on the average size of the particles and is sensitive to chemical treatment of the platinum surface. The spin–spin and spin–lattice relaxation times $T_1$ and $T_2$ changed on going from one region of the spectrum to another, but were the same for a given value of the magnetic field and for a given type of treatment of the surface, irrespective of the degree of dispersion of the specimens. The specimen with the largest platinum particles gave a narrow peak from metallic platinum.[57,58] After the specimens were treated with hydrogen or air, the spectra showed an intense peak with a chemical shift characteristic of diamagnetic platinum compounds. This peak was assigned to surface Pt atoms chemically combined with hydrogen or oxygen. Evidence in support of this assignment was provided by the long (~0.1 s) relaxation time $T_1$, whose dependence on temperature and on the field was different from that for metals.

For specimens of highly dispersed platinum on aluminium oxide after the chemisorption of carbon monoxide, the use of $^{13}C$ and $^{195}Pt$ double resonance made it possible to distinguish the signals from the Pt atoms in the surface layer and in the volume.[59] This is possible since irradiation of the specimen at the $^{13}C$ resonance frequency influences only the spectrum of those Pt atoms which are in direct proximity to C atoms. It was found that the magnitude of the spin–spin coupling constant between the carbon and platinum nuclei is similar to that of the corresponding constant for diamagnetic platinum carbonyl molecules. Thus carbon monoxide is bonded to deposited platinum through the carbon atom, as in platinum carbonyls.

### 5. $^{17}O$ NMR Studies of Oxides

Since oxide compounds are widely used as catalysts, the possibility of studying them by $^{17}O$ NMR is of considerable interest. The only oxygen isotope with a non-zero magnetic moment, $^{17}O$, has a very low natural abundance (0.037%). Until recently, therefore, $^{17}O$ NMR spectroscopic studies were carried out only for solutions and mainly using enriched specimens, and there were no published data on the $^{17}O$ NMR of crystalline specimens. Increase in the sensitivity of the method has made it possible to carry out routine measurements of the $^{17}O$ NMR spectra of solutions and to begin the $^{17}O$ NMR study of solid oxides.

The $^{17}O$ NMR spectra of MgO and $Ni_xMg_{1-x}O$ solid solutions with the natural concentration of the $^{17}O$ isotope were first reported in Ref.60. The chemical shift for oxygen in MgO was measured, and it was shown that the NMR parameters (line width, spin–lattice relaxation time) can be used to analyse the distribution of the paramagnetic $Ni^{2+}$ ions in the MgO lattice. In the analysis of enriched (enrichment in $^{17}O$ up to 20%) specimens of MgO, $SiO_2$, $\alpha$-$Al_2O_3$, and $CaMg.Si_2O_6$ [61] it was possible, using rotation at the magic angle, to resolve lines from structurally non-equivalent O atoms in the NMR spectra. Thus the spectrum of $CaMgSi_2O_6$ showed three lines from non-equivalent O atoms, whereas the $^{29}Si$ spectrum consisted of only a single line. The fact that the $^{17}O$ nucleus has a quadrupole moment makes it possible to obtain additional information on the symmetry of the environment of oxygen in the lattice by studying the quadrupole effects in the NMR spectra.

Thus the first studies of the $^{17}O$ NMR spectra of solid oxides demonstrate the possibilities provided by the method for structural studies based on the measurement of both the chemical shifts and the parameters of the quadrupole interaction.

### 6. $^{1}H$ NMR Studies of Surface OH Groups

The structure of the hydroxide covering of catalyst surfaces plays an important role in heterogeneous catalytic processes, so that it has been studied intensively by many methods, chiefly infrared spectroscopy.[62] A large number of studies have also been carried out by the traditional versions of NMR.[2] The use of the methods for decreasing the NMR line width makes it possible to observe separate lines from hydroxide protons of different chemical character, and this opens up the possibility of finding the relationship between the proton-donor properties of hydroxide groups and the nature of their chemical bond with the surface.

Thus the first papers[63,64] on the use of multi-phase sequences to study the OH groups of silica gel and aluminosilicates showed that this technique makes it possible to decrease the width and to measure the components of the tensor of the chemical shift for OH groups. For aluminosilicates, the free induction signal consisted of two components, one of which decreased more rapidly, and the other more slowly; the first component was assigned to OH groups bonded to aluminium, and the second to Si–OH groups. This made it possible to determine quantitatively the concentrations of OH groups of different types.

The proton resonance spectra of A-300 Aerosil dehydrated in a vacuum, with rotation at the magic angle, showed two lines with $\sigma$ = 2.0 p.p.m. and 2.9 p.p.m., corresponding to Si–OH and $Si(OH)_2$ groups respectively.[65] This made it possible to determine the concentrations of both types of group. When the specimen was kept in moist air, the spectrum showed new lines of two types, assigned[65] to water in hexagonal pores (signal with $\sigma$ = 1.1 p.p.m.) and water forming hydrogen bonds (signal with $\sigma$ in the range 4.2–4.4 p.p.m.).

For hygroscopic adsorbents and catalysts, the spectra of the OH groups are usually recorded in sealed ampoules, since atmospheric moisture adsorbed on the catalyst surface may distort the results considerably. The first studies of the NMR spectra of OH groups with rotation of the specimens

at the magic angle in sealed ampoules were described in Ref. 66. For silica gel it was possible to obtain a line width of 170 Hz, but the width was greater for the other specimens (~900 Hz for zeolites).

In the NMR spectra of the OH groups of HZSM-5 zeolites with different Si/Al ratios[68] without rotation of the specimen, the line width was ~4 kHz. With rotation of the specimen, the line width decreased by a factor of 6; this made it possible to resolve in the spectrum two lines with $\sigma = 1.4$ p.p.m. and 4.3 p.p.m. Since the intensity of the signal with $\sigma =$ 4.3 p.p.m. increased with increase in the concentration of aluminium in the zeolite, this line was assigned to OH groups chemically combined with aluminium. The line with $\sigma =$ 1.4 p.p.m. was assigned to Si–OH groups; this conclusion was confirmed by the fact that in the spectrum of silica gel the OH groups gave almost the same value of $\sigma$ (1.7 p.p.m.).[68] The spectra of amorphous aluminosilicates, including those of specimens with the same aluminium concentration as the HZSM-5 zeolites, did not show a line with $\sigma = 4.3$ p.p.m., corresponding to hydroxide groups joined to aluminium. This indicates that the concentration of these OH groups in zeolites is much higher than in amorphous aluminosilicates with the same composition. Phosphate catalysts contain several hydroxide groups of different types: P–OH and E–OH, where E is the second element in the phosphate. The lines with $\sigma$ in the range 3.1–4.4 p.p.m. are assigned to P–OH groups; the spectra of some specimens show lines due to P–OH groups forming a hydrogen bond, which displaces the signal of the OH groups to weak fields (the lines with $\sigma =$ 5.7 p.p.m. and 8 p.p.m. for $BPO_4$ and 5.8 p.p.m. for tin phosphate). The greatest shielding of the protons ($\sigma =$ −0.3 p.p.m.) is observed for calcium phosphate; this possibly reflects the highly basic nature of the Ca–OH groups.

Comparison of the chemical shifts of the OH groups and the charges on the protons.

| OH group | $\sigma$, p.p.m. | $q$, e (Ref.68) | OH group | $\sigma$, p.p.m. | $q$, e (Ref.68) |
|---|---|---|---|---|---|
| $H^+$ ion in the gas phase | 31 (Ref.67) | 0.0 | Si–OH | 1.7 | 0.72 |
| P–OH | 3.1 | 0.7 | Al–OH | 1.2 | 0.76 |
| Al–O(H)–Si | 4.3 | 0.71 | B–OH | 1.1 | 0.76 |

Notation: $\sigma$ is the chemical shift relative to TMS, and $q$ the relative density of the charge on the proton.

The chemical shift in $^1$H NMR spectra is the sum of three components, produced by the effects of the shielding of the protons by the electron cloud (the so-called electronic component), the magnetic anisotropy of the chemical bonds, and the polarisation of the electron clouds by the charges of neighbouring ions. The values of $\sigma$ for OH groups of different kinds have been compared[68] with the values of the charges on the protons of the surface OH groups, calculated by the MINDO/3 method, which usually gives an accurate description of the charge distribution; the results of the comparison are given in the Table. The Table shows that the signal tends to be displaced to a strong field with increase in the negative charge on the proton. This may indicate that the change in the chemical shift is determined to a large extent by the change in the electronic component.

The $^1$H NMR spectra of ZSM-5 zeolites after thermal vacuum treatment at 200 °C and 350 °C have been studied.[69] These specimens contain hydroxide groups of two types; the weak-field signal was assigned to the protons of the Si–O(H)–Al group, and the strong-field signal to the protons of the Si–OH group.

The state of the protons in zeolite cavities has been studied.[70] The proton resonance signal after a $\pi/2$ pulse in hydrated NaA, NaX, and NaY zeolites at room temperature consists of rapidly ($\lesssim$ 100 μs) and slowly (> 1 ms) damped components. The first component is assigned to the protons in β-cavities (cubo-octahedra); it was not clear whether the protons in these cavities belonged to water molecules or to OH groups. To investigate this question, sodalites, which contain only β-cavities, were studied. For these specimens, the signal contained only the rapidly damped component, and this made possible a more detailed study of the state of the protons in the β-cavities. It was found that the concentration of OH groups was only 0.5 per cubo-octahedron, and that they appear in the initial stage of the hydration of the zeolite after its activation at 400 °C. The number of OH groups does not increase with increase in the degree of filling of the zeolite cavities by water molecules, and is independent of temperature in the range between −150 °C and +150 °C. All the other protons belong to water molecules in the cubo-octahedra (~4 molecules per cubo-octahedron). The study of the temperature dependence of the spectra made it possible to follow the mobility of the water molecules.[70] In the comparatively short temperature range between −150 °C and 0 °C, the molecules undergo rapid anisotropic rotation; at a temperature above 0 °C the rotation becomes isotropic; and above 80–130 °C, translational movement of the water molecules between different cubo-octahedra takes place.

## IV. THE STUDY OF ADSORBED MOLECULES AND THEIR TRANSFORMATIONS

The high-resolution NMR spectra of adsorbed molecules can be obtained using the same methods of decreasing the line width as in the study of catalysts. The use of these methods is often made difficult, however, by the comparatively low concentration of adsorbed molecules. For this reason, in a number of cases, the NMR characteristics of chemisorbed species are obtained by recording the spectra under the conditions of the rapid exchange of molecules between the chemisorption centres and physical adsorption. A similar rapid-exchange procedure is widely used to study the complexes of reagents with metal-complex catalysts.[1] It makes it possible to determine the parameters of the low-intensity NMR spectra of chemisorbed species from the concentration dependence of the parameters of the overall averaged NMR spectrum of chemisorbed and physically adsorbed species. The intensity of this overall spectrum may be increased considerably by the high concentration of physically adsorbed species.

Rapid (on the NMR time scale) exchange between the chemisorbed and physically adsorbed states of molecules is encountered fairly frequently. The characteristic features of the analysis of NMR spectra under these conditions will be examined first, followed by an analysis of the results of NMR studies of specific adsorption and catalytic processes.

### 1. NMR Spectra with the Exchange of Molecules in the Adsorbed Layer

The principles of the analysis of NMR spectra with exchange in the adsorbed layer were developed in Refs. 71–76. It is assumed that on a catalyst surface, molecules are present either in the chemisorbed state, which is characterised by a chemical shift $\sigma_A$ and a lifetime $\tau_A$, or in a state of weak physical adsorption with a chemical shift $\sigma_0$ and a lifetime $\tau_0$. It is also assumed that exchange takes place between these two states as a result of thermal motion. For long lifetimes, that is when $\nu_0(\sigma_A - \sigma_0) \gg \tau_A^{-1}$ and $\nu_0(\sigma_A - \sigma_0) \gg \tau_0^{-1}$, where $\nu_0$ is the resonance frequency of the nucleus, the NMR spectrum consists of the superposition of the signals from the two states. For short lifetimes, if the conditions $\nu_0(\sigma_A - \sigma_0) \ll \tau_A^{-1}$ and $\nu_0(\sigma_A - \sigma_0) \ll \tau_0^{-1}$ are fulfilled, an averaged spectrum will be observed, in which the chemical shift is the average for the molecules in the two states.

If the surface has only one type of chemisorption centre and if the number of adsorption centres $N_A$ is much smaller than the total number of molecules on the surface $N$, the expression for the chemical shift $\sigma$ has the form

$$\sigma = \sigma_A \frac{KN_A}{1 + KN} \qquad (6)$$

where $K$ is the complex-formation constant. The measured dependence of $\sigma$ on $N$ can be used to determine $K$ and the product $\sigma_A N_A$.

The chemical shift for a molecule in an adsorbed layer is often measured relative to the position of the line of the same molecule in the gas. In this situation, the interpretation of the results of the measurements is influenced considerably by the choice of the value of the chemical shift $\sigma_0$ in the "free" state. The chemical shifts of the same molecules in liquids and gases differ considerably as a result of intermolecular van der Waals interactions and self-association.[77,78] In the general case, the greatest differences (5 p.p.m.) are observed for the nuclei situated at the periphery of the molecule. The values of the shifts for the gas phase in the $^{13}C$ NMR spectra in the great majority of cases are displaced to a strong field compared with liquids. In the study of the chemisorption of molecules, the value taken for $\sigma_A$ is often the value of the chemical shift for the same molecules on inert carriers (that is carriers with practically no chemisorption centres), for example silica gel. With this choice of the value of $\sigma_0$, it is possible simultaneously to compensate to a considerable extent the influence of the magnetic susceptibility of the catalyst on the magnitude of the chemical shift of the signal of the adsorbed molecules relative to the molecules in the gas. Experiments have shown that the differences in the chemical shifts as a result of the differences in the magnetic susceptibilities of silica gel and the catalyst (if it is diamagnetic) are usually small (~0.5 p.p.m.).

### 2. $^{13}C$ NMR Studies of the Adsorption of Hydrocarbons and CO

The use of the resonance of the $^{13}C$ nucleus (spin 1/2, natural abundance 1.1%) has a number of advantages over proton resonance. $^{13}C$ NMR spectra have a much greater (by a factor of 20–30) range of chemical shift values, that is they are much more sensitive to a change in the electronic state of the molecule. This often makes it possible to observe a change in chemical shifts in $^{13}C$ NMR spectra in cases where a displacement of the lines in the proton resonance spectrum cannot be detected. On the other hand, the magnetic moment of the $^{13}C$ nucleus is smaller by a factor of ~4 than that of the proton. As a result, there is a decrease in the contribution of dipole interaction to the line width. At the same time the dipole interaction between the $^{13}C$ nuclei is small, because of their low natural abundance, and the dipole interaction of these nuclei with protons can be decreased considerably by broad-band suppression of the spin–spin interaction. Thus the $^{13}C$ NMR spectra of adsorbed molecules have a much higher resolution than the $^{1}H$ NMR spectra. This feature has led to the extensive use of $^{13}C$ NMR spectroscopy to study adsorption, in spite of the fact that, because of the low natural abundance, the intensity of the signal from the $^{13}C$ nuclei is smaller by a factor of approximately $1.8 \times 10^{-4}$ than that from the protons, and the relaxation times, which are much greater than those for protons, require long times for the accumulation and recording of the spectra.

The present section describes the results of the study of the adsorption of hydrocarbon and CO molecules by NMR without rotation at the magic angle. This method makes it possible to study comparatively weak forms of adsorption, when the adsorbed molecules are still able to move (movement over the surface or rotation), so that they have comparatively narrow NMR lines.

The first $^{13}C$ NMR spectra of adsorbed molecules were reported in Refs. 79 and 80. The $^{13}C$ NMR spectra of adsorbed butenes and various other hydrocarbons have been studied.[79–84] A change in the chemical shifts and relaxation times was observed when butene isomers were adsorbed on zeolites.[80] The direction and magnitude of the shifts indicate that the electrons of the double bond take part in the interaction of the butenes with the surface active centres of the zeolites.

The spectra of toluene adsorbed on zeolites have been obtained.[82] The data on the chemical shifts of toluene and butenes adsorbed on zeolites were compared with the results of CNDO calculations. In the calculations it was assumed that the hydrocarbons interact with the sodium ions or OH groups of the zeolites. Agreement with experiment was not obtained, however, possibly because the quantum-chemical calculations were insufficiently accurate. The interaction of butenes with AgNaX and AgNaY zeolites has been studied,[83] and it was found that the chemical shifts are the same as those for the alkenes in aqueous solutions of silver salts. It was therefore concluded[83] that the butene molecules are adsorbed on the silver cation to form $\pi$-complexes. In Ref. 84, the $^{13}C$ NMR spectra were used for the first time to follow the isomerisation of but-1-ene into but-2-ene. Almost simultaneously, Gay[86] observed the spectra of carbon dioxide, ethylene, dichloroethane, ethanol, acetone, butenes, dimethyl ether, and hexane adsorbed on silica gel. In all cases the resolution of the $^{13}C$ NMR spectra was much better than that of the $^{1}H$ NMR spectra. For some molecules, changes in the chemical shifts (up to several p.p.m.) relative to the gas phase were observed.

$^{13}C$ NMR spectroscopy has been used[87] to study the adsorption of methane, carbon monoxide, acetylene, ethylene, propene, propyne, carbon oxide sulphide, propane, cyclopropane, and isobutane on NaA, NaX, NaY, and AgY zeolites and on silica gel. The influence of traces of iron in the catalysts on the line width of the adsorbed molecules was studied. At an iron concentration of $\sim 10^{-4}$ at.% it was possible to obtain very narrow lines (width ~10 Hz), and this made it possible to determine the changes in the chemical shifts (± 0.05 p.p.m.) and the spin–spin coupling constants (± 0.2 Hz) with a high accuracy. The magnitude of $\sigma$ was independent of the degree of covering. The shifts of the lines on adsorption on zeolites were attributed to interaction with surface centres—alkali metal cations and OH groups.

One of the main reasons for the change in the values of $\sigma$ for molecules in the adsorbed state is considered to be the influence of the electric field of the surface.[87] The decrease in the spin–spin coupling constant indicates an increase in the length of the C–H bonds in ethylene and propene when they are adsorbed on zeolites. Measurement of the temperature dependence of the line width and the spin–lattice relaxation time led to the conclusion that the mobility of the molecules in the adsorbed state is lower on HY zeolites than on NaY zeolites.

The spectra of a number of linear and cyclic alkenes adsorbed on zinc oxides have been studied.[88] For alkenes in whose molecules the double bond is readily accessible for interaction with surface atoms, the magnitude of $\sigma$ indicated that weak $\pi$-complexes are formed. In substituted alkenes there is steric hindrance to the formation of this bond. In Ref. 88, as in most early work, the dependence of the chemical shifts on coverage was not studied, so that the conclusions reached about the relative strength of the bonds formed by different alkenes with the active surface centres of zinc oxide (assumed to be $Zn^{2+}$ ions on the surface) require verification.

The adsorption of butenes on silicon and aluminium oxides has been studied;[89] a correlation was observed between the values of $\sigma$ and the quantity of OH groups on the catalyst surface. On the other hand, spectroscopic studies of the adsorption of butenes on silica gel modified with alkali showed that the alkenes interact not only with the OH groups and sodium ions but also with other centres of the silica gel surface, possibly oxygen anions.[90]

The adsorption of formic acid on titanium dioxide has been studied by $^{13}C$ and $^{1}H$ NMR.[91] Appreciable strong-field shifts of the $^{1}H$ NMR lines and weak-field shifts of the $^{13}C$ lines were observed, due to interaction with the surface paramagnetic $Ti^{3+}$ ions. The dependence of the values of $\sigma$ on the degree of covering of the surface, and EPR data on the number of adsorption centres, were used to determine the values of $\sigma_A$ and the spin densities at the protons and carbon nuclei of the surface complex. Quantum-chemical calculations of the transfer of spin density from the $Ti^{3+}$ ion to the $\pi$-orbitals of the adsorbed molecule[91] show that the experimental values of the spin densities are best explained by an adsorption model in which the structure of the formic acid molecule is distorted relative to its state in the gas phase—it loses its planar structure.

The possibility of observing the change in the concentration of each of the reaction products from the $^{13}C$ NMR spectra enables this method to be used to study the kinetics of the transformation of hydrocarbons on catalyst surfaces and to study the intermediate products of the catalytic reactions. It has been possible to follow the kinetics of the isomerisation of but-1-ene on tin–antimony catalysts from the change with time in the intensity of the lines in the $^{13}C$ NMR spectra from all the reaction products.[92] The kinetic data were used to propose a cyclic model of the surface complex whose geometry ensures the transformation of but-1-ene into but-2-ene and the *cis–trans* isomerisation of but-2-ene.

$^{13}C$ NMR has been used[93] to study the mechanism of the conversion of methanol and ethanol into hydrocarbons on ZSM-5 zeolite. Analysis of the $^{13}C$ NMR spectra made it possible to follow the sequence of transformations of the alcohols into hydrocarbons. All intermediate products were identified (ethers, alkenes, aromatic hydrocarbons, cyclic and saturated hydrocarbons) and a reaction scheme was proposed.

Because of the increase in interest in the study of the Fischer–Tropsch synthesis, an increasing number of studies of the mechanism of this reaction by $^{13}C$ NMR are being reported. The forms in which CO is adsorbed, and the nature of the intermediate products of the reaction of CO and $H_2$, have been investigated.

By using carbon monoxide enriched in the $^{13}C$ isotope (~90%), it has been possible to establish the nature of the species formed when CO or a CO + $H_2$ mixture is adsorbed on an $Rh/La_2O_3$ catalyst.[94]

The magnitude of the shift observed for CO adsorbed on $La_2O_3$ (180–250 p.p.m.) is typical of carbon atoms in metal carbonyls or in aldehyde groups; this indicates that carbonyl-like structures are formed. The $^{13}C$ NMR spectra of carbon monoxide adsorbed on $Rh/La_2O_3$ at 20 °C and 150 °C are also typical of carbonyl structures.[94] Heating these specimens to 200 °C leads to the formation of saturated hydrocarbons as a result of the reaction of the carbonyl species with the OH groups of the surface. In a similar experiment with $Rh/SiO_2$, the chief product was ethylene, and the degree of transformation of the carbonyls to the hydrocarbon was much lower than on $Rh/La_2O_3$.

For mixtures with $CO:H_2 = 1:3$ on an $Rh/La_2O_3$ catalyst, the reaction of CO with $H_2$ begins with the formation of carbonyl species with $\sigma$ = 180–150 p.p.m. Up to 80 °C, no other species were detected. Heating at 200 °C leads to the formation of alcohols. At 240 °C, the alcohols are dehydrated to give hydrocarbons (lines at 10–30 p.p.m.), which in turn are converted into methane at 260 °C.[94] At lower partial pressures of hydrogen ($CO:H_2 = 1:1$) and a temperature of 230 °C, large quantities of oxygen-containing compounds with carbonyl groups (lines with $\sigma \cong$ 180–220 p.p.m.) and compounds of the formate type (lines with $\sigma \cong$ 150–180 p.p.m.) are formed. With increase in temperature, saturated hydrocarbons predominate in the reaction products. These examples show that $^{13}C$ NMR can be used to study the intermediate products of the heterogeneous catalytic reactions between CO and $H_2$.

A study of the $^{13}C$ NMR spectra of CO and $CO_2$ adsorbed on zeolites[95] detected unusually large weak-field shifts of the signals (by ~30–80 p.p.m.) compared with gaseous CO. The shifts were observed after zeolite treatment leading to the displacement of aluminium (heating at a high temperature in a deep bed of the specimen); it was therefore concluded that the CO molecules interact with Lewis centres, that is with the aluminium atoms displaced from the zeolite lattice. These effects were not observed for $CO_2$. A model *ab initio* calculation of the interaction of CO with an isolated $Al^{3+}$ ion[96] showed that the potential energy on the surface has two minima, which correspond to the attachment of a CO to an $Al^{3+}$ ion via the carbon atom or via the O atom, with approximately equal stabilisation energies. Comparison of the results of the calculation of the chemical shift tensors with the experimental data led to the conclusion that in the decationated zeolites the addition of CO to $Al^{3+}$ takes place preferentially via the O atom.

A study of the state of CO adsorbed on $Rh/Al_2O_3$[97,98] detected species of two types, which give overlapping $^{13}C$ NMR spectra; these spectra differ, however, in their spin–lattice relaxation times. In this case, NMR supplements the results obtained by infrared spectroscopy (which does not detect two forms of adsorbed CO).

The methods of the high-resolution $^{13}C$ NMR spectroscopy of solids, involving suppression of the dipole interaction with protons, cross polarisation, and rotation of the specimens at the magic angle, are now beginning to be used increasingly to study strongly adsorbed molecules.

$^{13}C$ NMR with cross polarisation and suppression of the dipole and scalar interactions with protons has been used[99] to study the interactions of methanol, toluene, and ethylbenzene with modified zeolites of type X, used as catalysts for the synthesis of styrene. The results[99] show that the

introduction of alkali metal cations (NaX and CsX) leads to a change in the geometry of the zeolite cavities and the composition of the intermediate reaction products. The change in the size of the "windows" in the zeolites with change in the nature of the alkali metal influences the mobility of the adsorbed molecules (revealed by a change in the NMR line width) and the geometry of the intermediate state (revealed by the formation of different intermediate reaction products, detected from the characteristic shifts in the NMR spectra). Thus on NaX zeolite the dehydration of methanol predominates, whereas on CsX zeolite, dehydrogenation predominates. Formaldehyde is converted into dimethyl ether on NaX, and into methanol on CsX.

The chemisorption of methanol on magnesium oxide has been studied by cross polarisation.[100] The $^{13}C$ NMR spectra of adsorbed methanol had axial symmetry. Comparison with the spectra of potassium, calcium, and magnesium methoxides made it possible to assign the lines obtained after the adsorption of 6 μmole $m^{-2}$ methanol to surface magnesium methoxides, firmly bound to the catalyst surface. At high degrees of coverage, mobile methanol molecules joined to OH groups by hydrogen bonds are formed on the surface.

$^{13}C$ NMR has been used[101] to study the conversion of methanol on NaGeX-300 zeolite, which has a structure similar to that of faujasite. The formation of dimethyl ether and partial methoxylation of the surface were detected at 300 °C. In the presence of water, the surface methoxy groups are readily converted into methanol at 25 °C.

Important information can also be obtained by analysing the form of the lines in the $^{13}C$ NMR spectra. In the adsorption of benzene on NaY zeolite, the line width reaches a maximum after the adsorption of four benzene molecules for every large cavity.[102] This was taken[102] as indicating that benzene reacts with four sodium ions in a large cavity.

An analysis of the form of the lines in the spectra of CO, $CO_2$, $CS_2$, and COS adsorbed on zeolites has been used to identify the probable centres on which these molecules are adsorbed in mordenites.[103] This identification can be carried out by studying (from the form of the NMR line) the characteristic features of the movement of the molecules in the zeolites. The molecules have a low mobility if their dimensions and the dimensions of the adsorption sites coincide, and are extremely mobile if the dimensions of the cavities in which adsorption takes place are much greater than the dimensions of the molecules. For example, the data obtained[103] for $CO_2$ adsorbed on Na-mordenite indicate that the zeolite contains molecules of three types: stationary, rotating anisotropically, and rotating isotropically. These results can be attributed to the adsorption of $CO_2$ molecules in three different positions: inside channels formed by large rings, inside channels formed by small rings, and on the external surface respectively. For K-, Cs-, and $NH_4$-mordenites, adsorption of gases in the small channels is not observed. These cations apparently themselves occupy the positions in the small channels, preventing the adsorption of other molecules in them.

### 3. The Use of Rotation at the Magic Angle to Study Adsorbed Molecules

The chief problem arising when rotation at the magic angle is used to study adsorbed molecules is associated with the need to rotate sealed glass ampoules. The strong centrifugal forces produced by rotation at a frequency of 2–4 kHz often lead to rupture of the ampoules. An ampoule and a rotor have been designed[104,105] for carrying out measurements with sealed ampoules at a rotation frequency of 2–2.5 kHz.

The efficiency of rotation of the specimen at the magic angle is illustrated in Fig.6, which gives the $^1H$ NMR spectra of propene adsorbed on $\gamma$-$Al_2O_3$.[104] In experiments without rotation of the specimen, the line width is ~500 Hz, which makes it impossible to resolve the lines from the protons of the CH and $CH_2$ groups. On rotation at the magic angle, the line width decreases by a factor of ~20, all the lines of propene are resolved, and the accuracy of the measurement of $\sigma$ is increased (to ±0.02 p.p.m.). For this system, all the resonance lines of both the $^1H$ NMR spectrum and the $^{13}C$ NMR spectrum are displaced to a weak field, compared with the spectrum of gaseous propene; the largest shift was observed for the CH group.

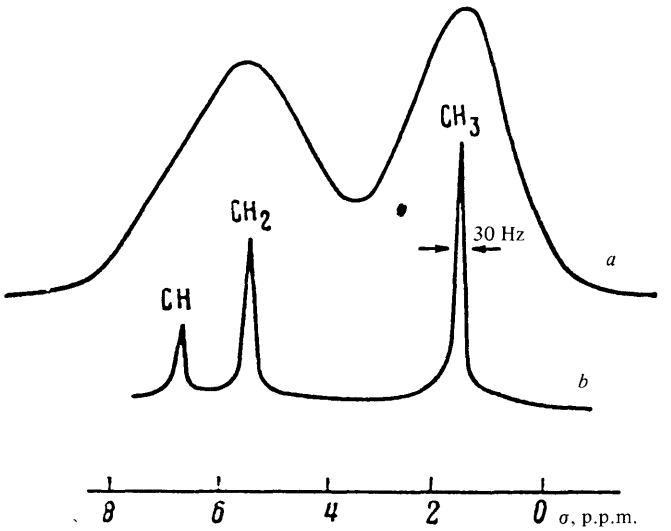



**Figure 6.** Influence of rotation at the magic angle on the $^1H$ NMR spectra of propene adsorbed on $\gamma$-$Al_2O_3$; the spectra were obtained: *a*) without rotation, *b*) with rotation at a frequency of 2 kHz.[104]

The dependence of the chemical shift on the degree of covering of the $\gamma$-$Al_2O_3$ surface by propene from the $^1H$ and $^{13}C$ NMR spectra is typical of rapid exchange between physically and chemically adsorbed alkene molecules. The dependence is effectively described by Eqn.(6), which corresponds to the chemisorption of propene on an active centre to give a 1:1 complex. Fig.7 gives the dependence of the chemical shift on the quantity of adsorbed propene.[105] The dependence of $\sigma$ on the degree of covering was used to find the complex-formation constant, whose value, as expected, was the same for all six lines in the $^1H$ and $^{13}C$ spectra. The values of the product of the chemical shift of the signal of the molecules in the adsorbed state and the number of chemisorption centres were also calculated. It was found that the complex-formation constant is independent of the temperature of preliminary vacuum treatment, whereas the product $\sigma_A N_A$ for all the lines increases with increase in the temperature of treatment (see Fig.7). This indicates that the propene chemisorption centres are most probably coordinatively unsaturated aluminium ions, the number of which increases with increase in the treatment temperature. A marked decrease in the values of the spin–spin coupling constants

$J(^{13}C-^{1}H)$ for all groups of chemisorbed propene compared with gaseous propene was also observed. For hydrocarbons, a decrease in the value of the constant $J(^{13}C-^{1}H)$ reflects a decrease in the strength of the C–H bond.[106] A comparison of the experimental values of σ and $J(^{13}C-^{1}H)$ with the results of MINDO/3 calculations for different forms of adsorption was used to obtain the most probable model of the chemisorption of propene on $\gamma$-$Al_2O_3$.[105] According to this model, the propene molecules are bonded to the surface by interactions of two types: between the π-electrons of the double bond of propene and the surface Al atom, and between the protons of the methyl group and the surface O atoms.

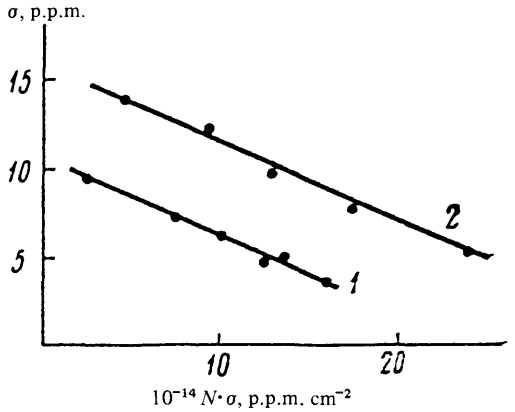



Figure 7. Plot of the chemical shift of propene adsorbed on $\gamma$-$Al_2O_3$ against $N.\sigma$ for different temperatures of treatment: *1*) 400 °C, *2*) 600 °C.[105]

Another example of the effective use of rotation at the magic angle to decrease the line widths for adsorbed molecules is provided by a study[107] of the $^{13}C$ NMR spectra of methane adsorbed on HZSM-5 zeolite. Rotation decreased the line widths considerably, making it possible to measure the change in not only the chemical shift but also the spin–spin coupling constant.[107] The signal from adsorbed methane is displaced to a weak field relative to methane in the gas phase. The spin–spin coupling constant decreases by ~10 Hz on adsorption. This indicates that a bond is formed between methane and surface centres, possibly leading to an increase in the length of the C–H bonds in the adsorbed molecule.

$^{13}C$ NMR with suppression of the spin–spin interaction with the protons has been used[108–110] to study the adsorption of ethylene enriched in the $^{13}C$ isotope on HZSM-5 zeolite at room temperature. The characteristic signal from ethylene (σ = 122 p.p.m.) was first observed. The intensity of this signal gradually decreased, and finally disappeared completely, indicating that ethylene is transformed into products which cannot be detected by NMR. The $^{13}C$ NMR spectra obtained with rotation of the specimens at the magic angle, immediately after the disappearance of the signal from ethylene, showed two lines at 28.8 p.p.m. and 13.5 p.p.m., assigned to aliphatic $CH_2$ and $CH_3$ groups respectively.[111] Both signals were broadened by dipole–dipole interaction between the carbon nuclei, but in spite of this, they showed a fine structure due to the presence of non-equivalent carbon atoms in the reaction products. Calculation of the relative intensity of the signals from the $CH_2$ and $CH_3$ groups[111] indicated that ethylene is converted into linear aliphatic hydrocarbons with 9–10 carbon atoms in the chain. The marked broadening of the lines and the fact that they cannot be observed without rotating the specimen at the magic angle indicate that the molecules of the reaction products form strong bonds with the zeolite.

$^{13}C$ NMR with rotation of the specimens at the magic angle and cross polarisation has also been used[112] to study the oligomerisation of alkenes on HZSM-5 zeolite. The chief products are linear oligomers at room temperature, and branched oligomers at high temperatures (~100 °C). This follows from a comparison of the values of σ with data for polymers with different structures. In contrast to this, on HY zeolites and H-mordenite, the alkenes are converted chiefly into branched oligomers at room temperature also. These differences are apparently due to the characteristic features of the structure of the HZSM zeolites, which have pores of smaller diameter.

## 4. The Study of the Adsorption on the Acidic Centres of Catalysts

Because of the important role of surface acidic centres in catalytic reactions, the adsorption of various molecules on these centres has been intensively studied for a long time by various physicochemical methods, mainly infrared spectroscopy.[113,114] Since $^{13}C$ NMR spectroscopy makes it possible to distinguish molecules in the free and adsorbed states, it has also been used to study surface acidic centres.[115–117]

The NMR spectra of a number of amines, including pyridine, aniline, and some of their derivatives, adsorbed on $SiO_2$, $Al_2O_3$, and an aluminosilicate, have been obtained.[115] On $SiO_2$, only a slight change in σ for the nuclei of the amines was observed, except for N,N-diethylaniline, for which an unusually large shift (–9 p.p.m.) of the signal of the C(4) carbon atom was observed; this may be due to a change in the geometry of the molecule on adsorption. The adsorption of amines on $Al_2O_3$ was accompanied by a much stronger interaction, but the spectra did not show the large chemical shifts usually observed when the corresponding amines are protonated in acidic solutions. This may be due to blocking of the strong acidic centres on the aluminium oxide surface. For the aluminosilicate, the values of σ were smaller than for the corresponding protonated amines in solution, and increased with decrease in the degree of covering of the surface. This last feature indicates that there is rapid exchange between the chemisorbed (protonated) and "free" (physically adsorbed) states of the amines. The rapid-exchange procedure was used[116] to study the adsorption of pyridine on silica gel treated with hydrochloric acid; the value of σ for chemisorbed pyridine was found to be close to the value for the pyridinium ion in aqueous solution.

In the simplest case, when there is exchange of an amine between two states, it is possible to write:[116]

$$\sigma = f_A\sigma_A + (1-f_A)\sigma_0 \qquad (7)$$

where σ is the observed chemical shift; $\sigma_0$ and $\sigma_A$ the chemical shifts for the free amine and for the amine combined with an acidic centre; and $f_A = N_A/N$ the proportion of amine molecules combined with acidic centres. If the amine can be combined with both Lewis and Bronsted acidic centres, generalisation of Eqn.(7) gives the expression

$$\sigma = f_H\sigma_H + f_L\sigma_L + (1-f_H-f_L)\sigma_0 \qquad (8)$$

where the subscripts "H" and "L" refer to Bronsted and Lewis centres respectively.

For the description of the dependence of $\sigma_H$ on the degree of covering of the surface in Ref.116 the value taken for $\sigma_H$ was that measured for the same amine in an acidic aqueous solution, the value taken for $\sigma_L$ was the value of the chemical shift for the complex of the amine with the Lewis acid $BF_3$, and the value taken for $\sigma_0$ was the value of the chemical shift for the amine adsorbed on $SiO_2$, which was assumed to have no surface acidic centres capable of protonating amines. Analysis (using Eqn.(8)) of the dependence of $\sigma$ on the degree of coverage for the adsorption of 4-ethylpyridine on the aluminosilicate showed good agreement between the values for the total number of acidic centres of the aluminosilicate obtained from the NMR spectra and from the adsorption of ammonia.

$^{13}C$ NMR has been used[118] to study the reaction of acetone with dehydroxylated and partly methylated silica gel specimens. An appreciable shift of the lines from the C=O group on the partly dehydroxylated specimens (by ~9 p.p.m. to a weak field) as a result of the formation of a hydrogen bond with OH groups was detected. The shifts for the methylated specimens were much smaller. The number of centres reacting with acetone was determined, and good agreement with the infrared spectroscopic data was obtained.

These studies were carried out using the standard high-resolution NMR procedure, which makes it possible to obtain well resolved spectra only when there is rapid movement of the adsorbed molecules on the surface. To obtain well resolved spectra for strongly adsorbed species, it is necessary to carry out the measurements at a fairly high temperature. This creates certain experimental difficulties, which can be overcome by using rotation of the specimens at the magic angle and cross polarisation to decrease the line widths. In Refs.119 and 120 these methods were used for the first time to study the adsorption of n-butylamine and pyridine on $\gamma$-$Al_2O_3$. The well resolved NMR spectra of n-butylamine showed the presence on the $\gamma$-$Al_2O_3$ surface of chemisorbed species of at least two types, due to the existence on the $\gamma$-$Al_2O_3$ surface of centres of two types interacting with the amine. Comparison with the spectra of the solid adducts of n-butylamine with HCl and $BCl_3$ made it possible to identify these centres as Bronsted and Lewis surface acidic centres. The separate observation of the lines from the amine adsorbed on these centres makes it possible in principle to use this method for the quantitative measurement of the numbers of acidic centres of different types.

The same procedure was used to study the spectra of pyridine adsorbed on $\gamma$-$Al_2O_3$. When the usual method of recording the spectra is used, pyridine gives broad poorly resolved lines even at increased temperatures and relatively high degrees of coverage. The use of rotation of the specimen at the magic angle combined with cross polarisation makes it possible to observe for pyridine adsorbed on $\gamma$-$Al_2O_3$ a completely resolved spectrum for all three non-equivalent carbon atoms. The values of $\sigma$ coincide with the corresponding values for liquid pyridine, indicating that the adsorbed pyridine molecules are weakly bound to the surface. When cross polarisation was used, lines of anomalous intensity were observed, and this can be attributed to the characteristic features of the dynamics of cross polarisation when the movement of the pyridine molecules in the adsorbed state is anisotropic. The results of the experiments agree with a model in which the pyridine molecule reacts with the surface via the nitrogen atom and rotates chiefly about the $C_2$ axis.

Extensive possibilities for the investigation of acidic centres are opened up by the study of the $^{15}N$ NMR spectra of adsorbed bases. Although the $^{13}C$ NMR spectra can be obtained at the natural concentration of the isotope, however, the much lower intensity of the signal from $^{15}N$ nuclei makes it necessary to use enriched specimens. The study of the $^{15}N$ NMR spectra of adsorbed bases is of particular interest, since both the protonation of these substances and their formation of a hydrogen bond with surface OH groups often take place directly via the nitrogen atom. As a result, the differences in the chemical shifts of the $^{15}N$ signals for the protonated and non-protonated molecules are greater than those for $^{13}C$ and $^{1}H$ nuclei. Few papers have yet been published, however, on the use of $^{15}N$ NMR to characterise surface acidic centres.

The $^{15}N$ NMR spectra of ammonia, trimethylamine, pyridine, and acetonitrile adsorbed on zeolites have been studied.[121] The spectra of pyridine on Y zeolite showed shifts (of ~90 p.p.m.) relative to the signal of pyridine adsorbed on $SiO_2$, indicating that pyridinium ions are formed. The number of OH groups interacting with pyridine was determined. The unusually large shifts obtained for a number of specimens were attributed to the formation of complexes with Lewis acid centres on the surface.

When pyridine was adsorbed on modified silica gels, the values of $\sigma$ in the $^{13}C$ NMR spectra remained practically unchanged, whereas the $^{15}N$ NMR spectra showed shifts of ~20 p.p.m. as a result of the formation of a hydrogen bond between pyridine and the OH groups of silica gel.[122] In the case of silica gel modified with phosphorus, the formation of pyridinium ions was observed, apparently as a result of the reaction with P–OH groups.

In a study of the $^{13}C$ and $^{15}N$ NMR spectra of acetonitrile adsorbed on zeolites containing $Li^+$, $Na^+$, $Rb^+$, $Cs^+$, and $Ag^+$ cations,[123] it was found that the exchange cations act as adsorption centres, leading to shifts of the signals in the $^{15}N$ NMR spectra. The $^{13}C$ and $^{15}N$ NMR spectra of pyridine adsorbed on an aluminosilicate have been studied[124] using cross polarisation and rotation at the magic angle. The reaction of pyridine with the surface centres of the aluminosilicate leads to a decrease in the difference in the chemical shifts in the $^{13}C$ NMR spectra for the $\alpha$- and $\beta$- and for the $\alpha$- and $\gamma$-carbon atoms of pyridine. Comparison of these values with the corresponding values for pyridine forming a hydrogen bond (a solution of pyridine in water) and for pyridine forming a coordinate bond with aluminium (the compound $C_5H_5NAl(C_2H_5)_3$) indicated that at low degrees of covering, pyridine is adsorbed chiefly on Lewis centres; the comparison also made it possible to calculate the proportion of pyridine combined with these centres, and to determine their absolute concentration. At high degrees of covering, most of the pyridine molecules form hydrogen bonds with OH groups.

An analysis of the $^{15}N$ NMR line widths indicated that there is movement of the adsorbed pyridine molecules on the surface.[124] Experiments on cross polarisation of the $^{13}C$ nuclei with different times of thermal contact between the spin systems showed that this movement is anisotropic. It apparently involves rotation of the pyridine molecule about the two-fold axis.

### 5. The Study of the Adsorption of Hydrogen

NMR is convenient for the study of adsorbed hydrogen, since it is highly sensitive to the electronic state and mobility of the adsorbed molecule. A large number of studies have been carried out by broad-line NMR or by nuclear magnetic relaxation to determine the correlation time of the movement of the molecules on the catalyst surface; these studies have been reviewed.[2,3] Recently, as a result of the development of spectrometers operating with high fields, it has become

possible to use NMR spectroscopy to measure the chemical shifts of adsorbed hydrogen.

A study of the spectra of hydrogen adsorbed on an $Rh/TiO_2$ catalyst detected two forms of hydrogen.[125] For the first, the value of $\sigma$ was close to that for TMS; this hydrogen is bound to rhodium. The second form of hydrogen has a very high mobility; this hydrogen reacts for a short time with surface paramagnetic $Ti^{3+}$ ions, leading to a strong-field shift of the signal. The mobile form is possibly produced by the dissociation of hydrogen molecules on rhodium with subsequent transfer of active hydrogen to the catalyst surface. After the combined adsorption of CO and $H_2$, the signal from the mobile hydrogen disappears, and the total absorption of hydrogen by the catalyst increases as a result of the formation of new species containing protons.[126]

A study of the $^1H$ NMR spectra of reduced copper–chromium catalysts for the partial hydrogenation of unsaturated hydrocarbons[127,128] indicated that the structure of the reduced catalysts contains an atomic form of hydrogen which brings about the selective hydrogenation of the hydrocarbons. The hydrogen species in these catalysts, which have the spinel structure, are situated close to the paramagnetic ions and have a low mobility, leading to marked broadening of their lines.

The adsorption of hydrogen on platinum has been studied.[129] Hydrogen may be present on platinum in two states: strongly (irreversibly) bound and weakly (reversibly) bound. On the basis of the first results, obtained in Ref.130 at high hydrogen pressures, it was possible in Ref.129 to detect two signals for platinum deposited on silica gel. The high-field signal with $\sigma \cong -50$ p.p.m. is due to irreversibly adsorbed hydrogen. This high value of $\sigma$ indicates a strong interaction between hydrogen and platinum. It is suggested that the atoms of this form of hydrogen are situated in the interstices of the surface platinum species. The signal close to that of TMS was assigned to hydrogen reversibly adsorbed on isolated platinum atoms.

A more detailed study[131] showed that for pure monodisperse platinum specimens deposited on $SiO_2$, the spectrum shows only the high-field signal, and the signal close to that of TMS is due to the presence of impurities in the specimens. It was also found that hydrogen in the presence of deposited platinum influences the spin–lattice relaxation of the Si–OH groups of the carrier. This effect is not observed for $SiO_2$ without platinum. It was suggested that the rate of the relaxation of the OH groups is increased by paramagnetic hydrogen atoms "flowing" from the platinum to the carrier. Further studies are required, however, for a more reliable explanation of the reasons for this effect.

Large strong-field shifts of the hydrogen signal, apparently due to the formation of hydride-like structures, have also been observed for other metals of the platinum group: Ru, Rh, Pd, Os, and Ir.[132] In the case of palladium, an averaged signal from chemisorbed hydrogen and hydrogen dissolved in palladium was observed. In the case of Ru and Os, the chemical shift for hydrogen was independent of the covering, but in the case of Rh it even increased with increase in the degree of covering of the surface by hydrogen. These effects have not yet been satisfactorily explained.

The adsorption of hydrogen on $Rh/Al_2O_3$ has been studied.[133] The $^1H$ NMR spectrum obtained consists of three lines: a line with $\sigma = -(10-15)$ p.p.m. from a surface hydride, a Pake doublet with a splitting of ~44 kHz from water molecules formed during the adsorption of hydrogen, and a narrow line from physically adsorbed hydrogen. Analysis of the spectrum shows that on the $Rh/La_2O_3$ catalyst, the activation of hydrogen involves hydride formation. The subsequent "flow" of activated hydrogen to the carrier may lead to partial reduction of the carrier surface. The water molecules formed in this process are firmly bound to metallic rhodium. Thus NMR spectroscopy makes it possible to observe the activation of hydrogen on metallic rhodium and its subsequent migration to the carrier.

The spectra of hydrogen adsorbed on $\gamma$-$Al_2O_3$ have been studied.[134] A single line was observed, due to rapid exchange between different forms of adsorbed hydrogen.

In a study of the adsorption of hydrogen on zinc oxide,[135] it was suggested that on the surface there is a weakly bound form $H_3^+$, produced by the reaction of hydrogen with a hydroxide group. This suggestion was based on the fact that the $^1H$ NMR spectrum showed a weak line with $\sigma \cong 15$ p.p.m. from the overall spectrum of the OH groups and physically adsorbed hydrogen; it requires verification.

While the present review was being prepared for publication, additional data appeared on the study of the local environment of silicon from the $^{29}Si$ NMR spectra[136–147] and the study of the acidic properties of the surface from the $^{31}P$ NMR spectra of phosphorus containing bases in HY zeolites.[148] High-resolution proton magnetic resonance has been used[149–151] to study the Bronsted acidic centres of amorphous aluminosilicates and zeolites. The high-resolution $^{17}O$ NMR spectra of solid oxides and zeolites have been studied.[152,153] Hydrocarbon complexes on catalyst surfaces have been studied.[154,155] There has recently been considerable interest in the high-resolution $^{27}Al$ and $^{31}P$ NMR study of aluminium phosphate catalysts with zeolitic structures.[156,157] Studies of heterogeneous catalysts and the processes taking place on their surfaces, carried out in the Soviet Union using the methods of the high-resolution NMR spectroscopy of solids, have been reviewed.[158]

---o0o---

The data given in the present review show that the production of a new generation of highly sensitive multi-nuclei NMR spectrometers and the development of various procedures for obtaining high-resolution NMR spectra for solid specimens have led to qualitative changes in the possibilities provided by NMR for the study of heterogeneous catalysis. This method can be used to carry out systematic studies of catalyst structures, the forms of adsorption of reagents, and their transformations in catalytic reactions.

The important role in the development of organic and inorganic chemistry, including homogeneous organic and metal-complex catalysis, now being played by the study of substances and processes in solution by the traditional method of high-resolution NMR is well known. The data presented in the present review indicate that in the near future, modern versions of the NMR method will begin to play a similar role in the development of heterogeneous catalysis.

## REFERENCES

1. K.I.Zamaraev, Kinetika i Kataliz, 1980, **21**, 295.
2. E.G.Derouane, J.Fraissard, J.J.Fripiat, and W.E.E.Stone, Catal.Rev., 1972, **7**, 121.
3. H.Pfeifer, NMR-Basic Principles and Progress, Vol.7, Springer, New York, 1972.
4. H.Pfeifer, Phys.Reports, 1976, **26C**, 293.
5. J.S.Waugh, L.M.Huber, and U.Haeberlen, Phys. Rev.Letters, 1968, **20**, 180.
6. M.Mehring, NMR-Basic Principles and Progress, Springer, New York, 1976.

7. U.Haeberlen, Adv.Magn.Resonance, 1976, Suppl.1, p.1.
8. R.W.Vaughan, Ann.Rep.Phys.Chem., 1978, **29**, 397.
9. E.R.Andrew, Progr.NMR Spectroscopy, 1971, **8**, 1.
10. P.Mansfeld, Progr.NMR Spectroscopy, 1971, **8**, 41.
11. A.Abragam, The Principles of Magnetic Resonance, Oxford University Press, London, 1961.
12. C.P.Slichter, Principles of Magnetic Resonance, Harper and Row, New York, 1963.
13. E.R.Andrew, A.Bradbury, and R.G.Eades, Nature, 1958, **182**, 1659.
14. E.R.Andrew, A.Bradbury, and R.G.Eades, Nature, 1959, **183**, 1802.
15. E.R.Andrew, L.F.Farnell, M.Firth, T.D.Gledhill, and I.Roberts, J.Magn.Resonance, 1969, **1**, 27.
16. E.R.Andrew, Phil.Trans.Roy.Soc., 1981, **A299**, 505.
17. E.R.Andrew and A.Jasinski, J.Phys., 1971, **C5**, 391.
18. W.K.Rhim, D.D.Elleman, and R.W.Vaughan, J.Chem. Phys., 1973, **59**, 3740.
19. W.K.Rhim, D.D.Elleman, L.B.Schreiber, and R.W.Vaughan, J.Chem.Phys., 1974, **60**, 4559.
20. A.Pines, M.G.Gibby, and J.S.Waugh, J.Chem.Phys., 1973, **59**, 569.
21. S.R.Hartmann and E.L.Hahn, Phys.Rev., 1962, **128**, 2048.
22. F.M.Lurie and C.P.Slichter, Phys.Rev., 1964, **133A**, 1108.
23. A.Pines, D.J.Ruben, S.Vega, and M.Mehring, Phys. Rev.Letters, 1976, **36**, 110.
24. S.Vega, T.W.Shattuck, and A.Pines, Phys.Rev. Letters, 1976, **37**, 43.
25. H.Hatanaka, T.Terao, and T.Hashi, J.Phys.Soc. Japan, 1975, **39**, 835.
26. H.Hatanaka and T.Hashi, J.Phys.Soc.Japan, 1975, **39**, 1139.
27. H.Hatanaka, T.Ozawa, and T.Hashi, J.Phys.Soc. Japan, 1977, **43**, 2089.
28. W.H.Jones, T.P.Graham, and R.G.Barnes, Phys. Rev., 1963, **132**, 1898.
29. V.M.Mastikhin, O.V.Lapina, V.N.Krasil'nikov, and A.A.Ivakin, React.Kinet.Catal.Letters, 1984, **24**(1–2), 119.
30. V.M.Mastikhin, V.M.Nekipelov, and K.I.Zamaraev, Kinetika i Kataliz, 1982, **23**, 1323.
31. V.M.Mastikhin, O.V.Lapina, and L.G.Simonova, React. Kinet.Catal.Letters, 1984, **24**(1–2), 127.
32. V.M.Mastikhin, O.V.Lapina, and L.G.Simonova, React.Kinet.Catal.Letters, 1984, **26**(3–4), 431.
33. J.W.Akitt, Ann.Rep.NMR, 1973, **5A**(4), 465.
34. D.Müller, W.Gessner, and A.-R.Grimmer, Z.Chem., 1977, **12**, 453.
35. A.Samoson, E.Kundla, and E.Lippmaa, J.Magn. Resonance, 1982, **49**, 350.
36. A.Samoson and E.Lippmaa, Chem.Phys.Letters, 1983, **100**, 205.
37. A.Samoson and E.Lippmaa, Phys.Rev., 1984, **28B**, 6567.
38. R.Tycko, Phys.Rev.Letters, 1983, **51**, 775.
39. V.M.Mastikhin, O.P.Krivoruchko, B.P.Zolotovskii, and R.A.Buyanov, React.Kinet.Catal.Letters, 1981, **18**(1–2), 117.
40. D.Freude, T.Fröhlich, H.Pfeifer, and G.Scheler, Zeolites, 1983, **3**, 171.
41. V.Bosacek, D.Freude, T.Fröhlich, H.Pfeifer, and H.Schmiedel, J.Coll.Interface Sci., 1982, **85**, 502.
42. J.Uytterhoeven, L.G.Christner, and W.K.Hall, J.Chem.Phys., 1965, **69**, 2177.
43. W.Loewenstein, Amer.Mineral., 1954, **39**, 92.
44. G.E.Maciel and D.W.Sindorf, J.Amer.Chem.Soc., 1980, **102**, 760.
45. D.W.Sindorf and G.E.Maciel, J.Amer.Chem.Soc., 1983, **105**, 1487.
46. E.T.Lippmaa, M.Mägi, A.Samoson, G.Engelhardt, and A.-R.Grimmer, J.Amer.Chem.Soc., 1980, **102**, 4889.
47. G.Engelhardt, D.Zeigan, E.T.Lippmaa, and M.Mägi, Z.anorg.allgem.Chem., 1983, **468**, 80.
48. J.M.Thomas, L.A.Bursill, E.A.Lodge, A.K.Cheetham, and C.A.Fyfe, Chem.Communs., 1981, 276.
49. J.Klinowski, J.M.Thomas, C.A.Fyfe, and J.S.Hartman, J.Phys.Chem., 1981, **85**, 2590.
50. M.T.Melchior, D.E.W.Vaughan, and A.J.Jacobson, J.Amer.Chem.Soc., 1982, **104**, 4859.
51. G.Engelhardt, U.Lohse, E.T.Lippmaa, M.Tarmak, and M.Mägi, Z.anorg.allgem.Chem., 1981, **482**, 49.
52. V.M.Mastikhin, A.A.Shubin, V.M.Nekipelov, and K.I.Zamaraev, Kinetika i Kataliz, 1983, **24**, 756.
53. G.Engelhardt, U.Lohse, V.Patzelova, M.Mägi, and E.T.Lippmaa, Zeolites, 1983, **3**, 233.
54. G.Engelhardt, U.Lohse, V.Patzelova, M.Mägi, and E.T.Lippmaa, Zeolites, 1983, **3**, 239.
55. G.Engelhardt, U.Lohse, A.Samoson, M.Mägi, M.Tarmak, and E.T.Lippmaa, Zeolites, 1982, **2**, 59.
56. J.B.Nagy, Z.Gabelica, E.G.Derouane, and P.A.Jacobs, Chem.Letters, 1982, 2003.
57. C.P.Slichter, Surface Sci., 1981, **106**, 382.
58. C.D.Makowka, C.P.Slichter, and J.H.Sinfelt, Phys. Rev.Letters, 1982, **49**, 379.
59. H.T.Stokes, C.D.Makowka, P.K.Wang, S.L.Rudaz, C.P.Slichter, and J.H.Sinfelt, J.Mol.Catal., 1983, **20**, 321.
60. M.A.Fedotov and G.F.Gerasimova, React.Kinet.Catal. Letters, 1983, **22**(1–2), 113.
61. S.Schramm, R.J.Kirkpatrick, and E.Oldfield, J.Amer. Chem.Soc., 1983, **105**, 2483.
62. A.V.Kiselev and V.I.Lygin, "Infrakrasnye Spektry Adsorbirovannykh Molekul" (The Infrared Spectra of Adsorbed Molecules), Izd.Nauka, Moscow, 1972.
63. R.W.Vaughan, L.B.Schreiber, and J.A.Schwartz, II Symp.on Magnetic Resonance in Colloid and Interface Science, San Francisco, 1976, Prep.No.24.
64. L.B.Schreiber and R.W.Vaughan, J.Catal., 1975, **40**, 226.
65. E.T.Lippmaa, A.V.Samoson, V.V.Brei, and Yu.I.Gorlov, Dokl.Akad.Nauk SSSR, 1981, **259**, 403.
66. D.Freude, M.Hunger, and H.Pfeifer, Chem.Phys. Letters, 1982, **91**, 307.
67. A.Carrington and A.D.McLachlan, Introduction to Magnetic Resonance, Harper, New York, 1967.
68. I.L.Mudrakovskii, V.M.Mastikhin, N.S.Kotsarenko, L.G.Karakchiev, A.G.Pel'menshchikov, and K.I.Zamaraev, React.Kinet.Catal.Letters.
69. K.F.M.G.J.Scholle, W.S.Veeman, J.G.Post, and J.H.C.van Hooff, Zeolites, 1983, **3**, 215.
70. H.Ernst, H.Pfeifer, and S.P.Zhdanov, Zeolites, 1983, **3**, 209.
71. V.Yu.Borovkov and V.B.Kazanskii, Kinetika i Kataliz, 1972, **13**, 1356.
72. V.B.Kazanskii, V.Yu.Borovkov, and G.M.Zhidomirov, J.Catal., 1975, **39**, 205.
73. V.Yu.Borovkov and V.B.Kazanskii, Kinetika i Kataliz, 1974, **15**, 705.
74. V.Yu.Borokov, G.M.Zhidomirov, and V.B.Kazanskii, Zhur.Strukt.Khim., 1975, **16**, 308.
75. C.L.Kibby, V.Yu.Borovkov, V.B.Kazanskii, and W.K.Hall, J.Catal., 1977, **46**, 275.
76. T.Bernstein, P.Fink, D.Michel, and H.Pfeifer, J.Coll. Interface Sci., 1981, **84**, 310.

77. B.Tiffon and D.Cans, J.Magn.Resonance, 1977, **27**, 147.
78. I.D.Gay and J.F.Kriz, J.Phys.Chem., 1978, **82**, 319.
79. D.Deininger and D.Michel, Wiss.Z.Karl-Marx-Univ. Leipzig, Math.Naturw.Reihe, 1975, **22**, 55.
80. D.Michel, Surface Sci., 1974, **42**, 453.
81. D.Geschke, W.D.Hoffmann, and D.Deininger, Surface Sci., 1976, **57**, 559.
82. D.Deininger, D.Geschke, and W.D.Hoffmann, Z.phys.Chem.(Leipzig), 1974, **255**, 273.
83. D.Michel, W.Meiler, and D.Hoppach, Z.phys.Chem. (Leipzig), 1974, **255**(3), 509.
84. D.Michel, W.Meiler, and H.Pfeifer, J.Mol.Catal., 1975, **1**, 85.
85. Note. Reference 85 omitted in Russian paper (Ed.of Translation).
86. I.D.Gay, J.Phys.Chem., 1974, **78**, 38.
87. D.Z.Denney, V.M.Mastikhin, S.Namba, and J.Turkevich, J.Phys.Chem., 1978, **82**, 1752.
88. I.T.Ali and I.D.Gay, J.Phys.Chem., 1981, **85**, 1251.
89. J.F.Kriz and I.D.Gay, J.Phys.Chem., 1976, **80**, 2951.
90. I.D.Gay, J.Phys.Chem., 1975, **79**, 2145.
91. M.A.Enriquez and J.P.Fraissard, J.Catal., 1982, **74**, 89.
92. J.B.Nagy, A.Abou-Kais, M.Guelton, J.Harmel, and E.G.Derouane, J.Catal., 1982, **73**, 1.
93. E.G.Derouane, J.B.Nagy, P.Dejaifve, J.H.C.Van Hooff, B.P.Spekman, J.C.Vedrine, and C.Naccache, J.Catal., 1978, **53**, 40.
94. V.L.Kuznetsov, A.V.Romanenko, I.L.Mudrakovskii, V.M.Mastikhin, and Yu.I.Ermakov, React.Kinet. Catal.Letters, 1984, **25**(1–2), 147.
95. A.Michael, W.Meiler, D.Michel, and H.Pfeifer, Chem. Phys.Letters, 1981, **84**, 30.
96. T.Weller, W.Meiler, A.Michael, H.J.Koehler, H.Lischka, and R.Hoeller, Chem.Phys., 1962, **72**, 155.
97. T.M.Duncan, J.T.Yates, and R.W.Vaughan, J.Chem. Phys., 1979, **71**, 3129.
98. T.M.Duncan, J.T.Yates, and R.W.Vaughan, J.Chem. Phys., 1980, **73**, 975.
99. M.D.Sefcik, J.Amer.Chem.Soc., 1979, **101**, 2164.
100. I.D.Gay, J.Phys.Chem., 1980, **84**, 3230.
101. E.G.Derouane, P.Dejaifve, and J.B.Nagy, J.Mol. Catal., 1978, **3**, 453.
102. V.Yu.Borovkov, W.K.Hall, and V.B.Kazanskii, J.Catal., 1978, **51**, 437.
103. M.D.Sefcik, J.Schaefer, and E.O.Stejskal, Magnetic Resonance in Colloid and Interface Science, ACS Symposium Series. Washington, 1976, p.34.
104. V.M.Mastikhin and I.L.Mudrakovskii, React.Kinet. Catal.Letters, 1982, **20**, 351.
105. V.M.Mastikhin, I.L.Mudrakovskii, A.G.Pel'menshchikov, and G.M.Zhidomirov, Surface Sci., 1984, **144**, 550.
106. J.W.Emsley, J.Feeney, and L.H.Sutcliffe, High Resolution Nuclear Magnetic Resonance Spectroscopy, Pergamon Press, New York, 1966.
107. I.L.Mudrakovskii, S.S.Shepelev, V.M.Mastikhin, K.G.Ione, K.I.Zamaraev, and G.K.Boreskov, Kinetika i Kataliz, 1984, **25**, 766.
108. V.Bolis, J.C.Vedrine, J.P.van den Berg, J.P.Wolthuizen, and E.G.Derouane, J.Chem.Soc. Faraday Trans.I, 1980, **76**, 1606.
109. J.P.Wolthuizen, J.P.van den Berg, and J.H.C.van Hooff, Catalysis by Zeolites. Elsevier, Amsterdam, 1980, p.85.
110. J.C.Vedrine, P.Dejaifve, C.Naccache, and E.G.Derouane, Proc.VII Int.Congress on Catalysis (Tokyo, 1981). Elsevier, Amsterdam, 1981, p.724.
111. E.G.Derouane, J.P.Gilson, and J.B.Nagy, J.Mol. Catal., 1981, **10**, 331.
112. J.P.Van den Berg, J.P.Wolthuizen, A.D.H.Clague, G.R.Hays, R.Huis, and J.H.C.van Hooff, J.Catal., 1983, **80**, 130.
113. L.H.Little, "Infrared Spectra of Adsorbed Species" (Translated into Russian), Izd.Mir, Moscow, 1969.
114. K.Tanabe, "Solid Acids and Bases" (Translated into Russian), Izd.Mir, Moscow, 1973.
115. I.D.Gay and S.Liang, J.Catal., 1976, **44**, 306.
116. I.D.Gay, J.Catal., 1977, **48**, 430.
117. S.Liang and I.D.Gay, J.Catal., 1980, **66**, 294.
118. T.Bernstein, D.Michel, and H.Pfeifer, J.Coll.Interface Sci., 1981, **84**, 310.
119. W.H.Dawson, S.W.Kaiser, P.D.Ellis, and R.R.Inners, J.Amer.Chem.Soc., 1981, **103**, 6780.
120. W.H.Dawson and S.W.Kaiser, J.Phys.Chem., 1982, **86**, 867.
121. D.Michel, A.Germanus, and H.Pfeifer, J.Chem.Soc., Faraday Trans.I, 1982, **78**, 237.
122. T.Bernstein, L.Kitaev, D.Michel, H.Pfeifer, and P.Fink, J.Chem.Soc., Faraday Trans.I, 1982, **78**, 761.
123. I.Juenger, W.Meiler, and H.Pfeifer, Zeolites, 1982, **2**, 310.
124. G.E.Maciel, J.F.Haw, I.S.Chuang, B.L.Hawkins, T.A.Early, D.R.McKay, and L.Petrakis, J.Amer. Chem.Soc., 1983, **105**, 5529.
125. T.M.Apple, P.Gajardo, and C.Dybowski, J.Catal., 1981, **68**, 103.
126. T.M.Apple and C.Dybowski, 1981, **71**, 316.
127. C.F.Aissi, M.Daage, G.Wroebel, M.Guelton, and J.P.Bonnelle, Applied Catal., 1982, **3**, 187.
128. C.F.Aissi, M.Daage, M.Guelton, J.P.Bonnelle, J.B.Nagy, and E.G.Derouane, J.Catal., 1982, **76**, 231.
129. J.L.Bonardet, L.C.Menorval, and J.Fraissard, Proc. VI Congress on Catalysis. Chem.Soc.Publ., London, 1976, prepr.22.
130. T.Ito, T.Kadowaki, and T.Toya, Japan J.Appl.Phys. Suppl.2, 1974, Pt.2, 257.
131. T.C.Sheng and I.D.Gay, J.Catal., 1981, **71**, 119.
132. T.C.Sheng and I.D.Gay, J.Catal., 1982, **77**, 53.
133. V.L.Kuznetsov, A.V.Romanenko, I.L.Mudrakovskii, V.M.Mastikhin, and Yu.I.Yermakov, React.Kinet. Catal.Letters, 1984, **25**(1–2), 137.
134. A.C.Cirillo, Jr., J.M.Dereppe, and W.K.Hall, J. Catal., 1980, **61**, 170.
135. M.Watanabe and T.Ito, Japan J.Appl.Phys., 1980, **19**, 1863.
136. C.A.Fyfe, et al., Angew.Chem., 1983, **2**, 259.
137. J.Klinowski, Progress in NMR Spectroscopy, 1984, **16**, 237.
138. G.R.Hays, W.A.van Erp, N.C.M.Alma, P.A.Couperus, R.Huis, and A.E.Wilson, Zeolites, 1984, **4**, 377.
139. C.M.Schramm, B.H.W.De Jong, and V.Parziale, J.Amer.Chem.Soc., 1984, **106**, 4396.
140. C.A.Fyfe, et al., J.Amer.Chem.Soc., 1984, **106**, 4435.
141. P.A.Diddams, J.M.Thomas, W.M.Jones, J.A.Ballantine, and J.H.Purnell, Chem.Communs.1984, 1340.
142. J.M.Thomas, J.Mol.Catal., 1984, 27, 59.
143. J.B.Nagy, Z.Gabeliva, G.Debras, P.Bodart, E.G.Derouane, and P.A.Jacobs, 1983, 20, 327.

144. A.R.Grimmer and R.Radeglia, Chem.Phys.Letters, 1984, **106**, 262.
145. J.M.Thomas, J.Klinowski, S.Ramdas, B.K.Hunter, and D.T.B.Tennakoon, J.Chem.Phys., 1983, **102**, 158.
146. C.A.Fyfe, G.C.Gobby, and G.J.Kennedy, J.Phys. Chem., 1984, **88**, 3248.
147. C.A.Fyfe, G.C.Gobby, and G.J.Kennedy, J.Phys. Chem., 1985, **89**, 277.
148. W.P.Rothwell, W.X.Shen, and J.H.Lunsford, J.Amer. Chem.Soc., 1984, **106**, 2452.
149. M.Hunger, D.Freude, H.Pfeifer, H.Bremer, M.Jank, and K.-P.Wendlandt, Chem.Phys.Letters, 1983, **100**, 29.
150. D.Freude, M.Hunger, and H.Pfeifer, Chem.Phys. Letters, 1984, **105**, 427.
151. K.F.M.G.J.Scholle, A.P.M.Kentgens, W.S.Veeman, P.Frenken, and G.P.M.van der Velden, J.Phys. Chem., 1984, **88**, 5.
152. S.Schramm and E.Oldfield, J.Amer.Chem.Soc., 1984, **106**, 2502.
153. S.Schramm, R.J.Kirkpatrick, and E.Oldfield, J.Amer.Chem.Soc., 1983, **105**, 2483.
154. V.A.Bell, R.F.Carver, C.R.Dybowski, and H.S.Gold, J.Chem.Soc., Faraday Trans.I, 1984, **80**, 831.
155. T.M.Duncan, P.Winslow, and A.T.Bell, Chem.Phys. Letters, 1983, **102**, 163.
156. C.S.Blackwell and R.L.Patton, J.Phys.Chem., 1984, **88**, 6135.
157. D.Müller, E.Jahn, B.Fahlke, G.Ladwig, and U.Haubenreisser, Zeolites, 1985, **5**, 53.
158. K.I.Zamaraev and V.M.Mastikhin, Colloids and Surface, 1984, **12**, 401.

Institute of Catalysis,
Siberian Branch,
Academy of Sciences of the
USSR, Novosibirsk